AD-A055 225 AIR FORCE INST OF TECH WRIGHT-PATTERSON AFB OHIO SCH--ETC F/G 17/4
AN APPLICATION OF SYNCHRONIZED PSEUDO-RANDOM NOISE TO RADAR JAM--ETC(U)
JAN 78 F E MOLINET

UNCLASSIFIED AFIT/GE/EE/78-12 NL

1 OF 2
AD
A055225

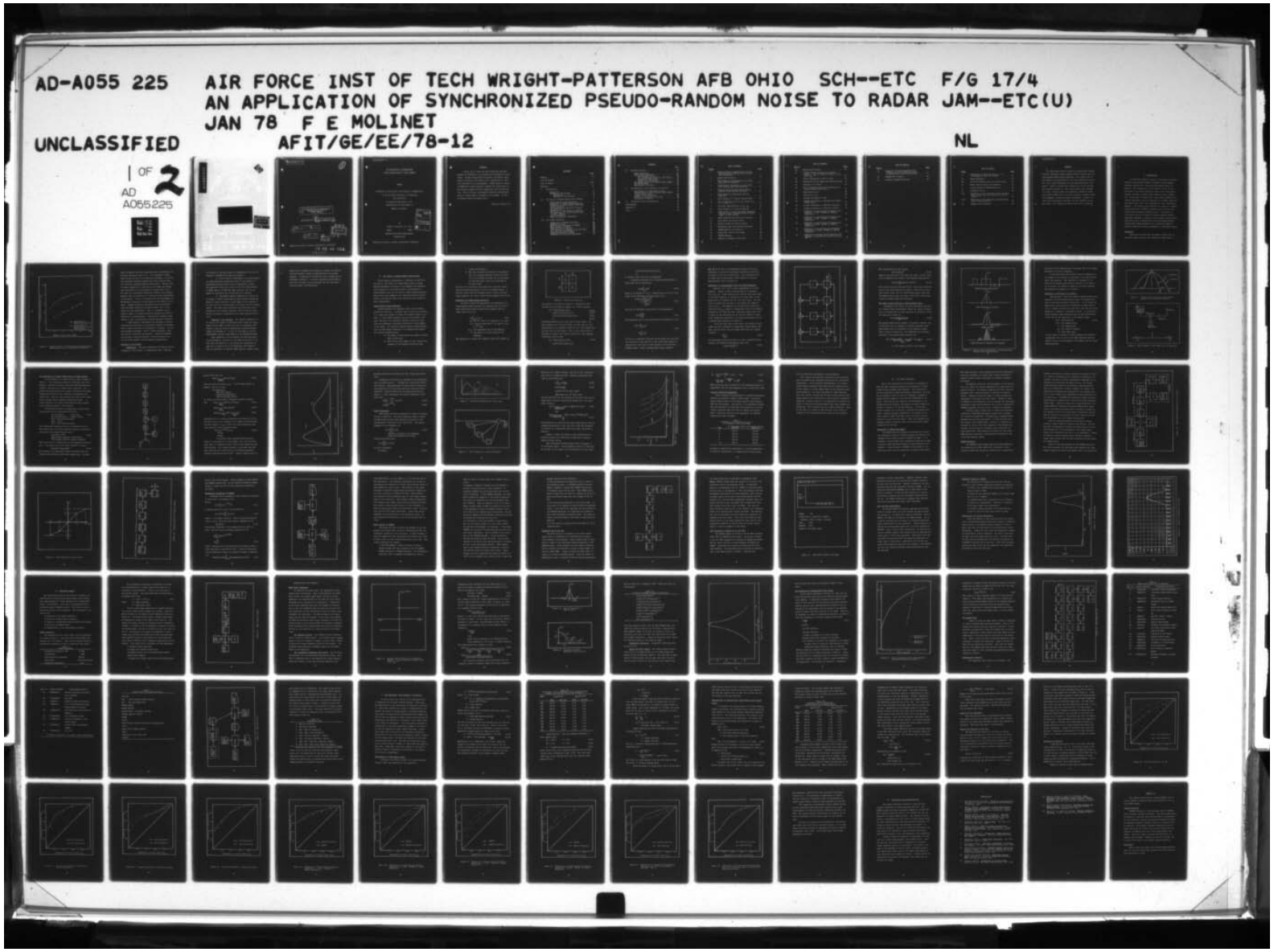

(14) AFIT/GE/EE/78- 12

(1)

(6) AN APPLICATION OF SYNCHRONIZED PSEUDO-RANDOM NOISE TO RADAR JAMMING.

(10)

AFIT/GE/EE/78-12 Fausto E. Molinet, Jr.
Major USAF

(9) Master's Thesis,

(11) Jan 78

(12) 102 p.

Approved for public release; distribution unlimited.

AFIT/GE/EE/78-12

AN APPLICATION OF SYNCHRONIZED PSEUDO-RANDOM NOISE TO RADAR JAMMING

THESIS

Presented to the Faculty of the School of Engineering

of the Air Force Institute of Technology

Air University

in Partial Fulfillment of the

Requirements for the Degree of

Master of Science

by

Fausto E. Molinet, Jr., B.S.

Major USAF

Graduate Electrical Engineering

January 1978

Approved for public release; distribution unlimited.

Preface

I would like to thank the many people who provided support and assistance to me during the development of this thesis. Captain Gregg Vaughn my advisor, and Doctor David Berrie, my sponsor, provided me with a great deal of technical assistance and encouragement. Robert Hancock, author of RADSIM was always willing to explain the intricacies of his computer program and make suggestions for its modification. My wife Denise, and daughter Francine suffered many hours of benign neglect throughout this program. To all - my undying thanks and appreciation.

Fausto E. Molinet, Jr.

Contents

Contents

List of Figures

List of Figures

List of Figures

List of Tables

Abstract

In 1974 Doctor David W. Berrie of Aeronautical Systems Division, proposed a radar jamming waveform derived from filtered pseudo-random binary sequences. The running time of the sequence is synchronized to the pulse repitition rate of the victim radar and defeats the post detection pulse integrator. Berrie's results were derived from theory and analog computer simulation. This study applies that waveform to a radar receiver model incorporating a DICKE-FIX (wideband limiter) ECCM device and uses a digital computer simulation (RADSIM) to determine radar performance. Berrie's results were essentially confirmed, and the DICKE-FIX device was found to be ineffective against this form of jamming.

I. Introduction

In 1974 Doctor David W. Berrie of Aeronautical Systems Division, USAF Systems Command, proposed a radar jamming waveform, derived from filtered pseudo-random binary sequences. The running time of the sequence was to be synchronized to the pulse repetition rate of the victim radar and was intended to defeat a post-detection pulse integrator. He was able to demonstrate, using analog computer simulation techniques, that the probability of target detection was reduced when this form of jamming was used, as shown in Figure 1. The analysis was conducted on a model of a simple search radar with a 127KHZ IF bandwidth and no Electronic Counter Counter Measures (ECCM) devices. The purpose of this thesis will be to adapt an existing digital computer simulation (RADSIM) to analyze a search radar incorporating ECCM devices and to demonstrate that synchronized pseudo-random noise jamming (SPRNJ) will be effective against a specific ECCM device known as DICKE-FIX, a wide-band limiter.

Background

Electronic warefare (EW) has played a major role in military operations since the beginning of World War II,

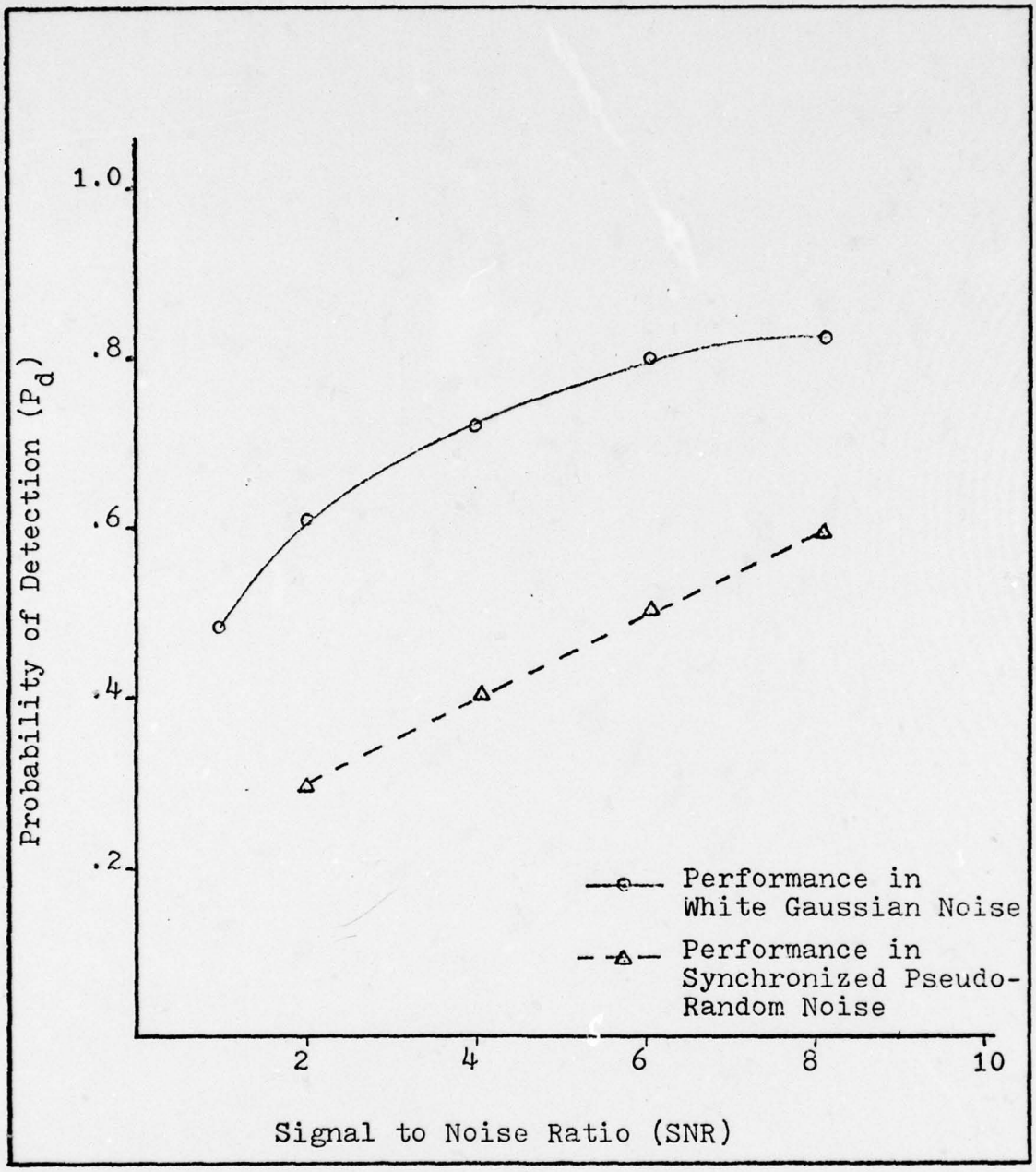

Figure 1. Relative Effect of Random Noise And Synchronized Pseudo-Random Noise of Detection Probability

which introduced the first large scale use of electronics in military operations (Ref 1:1-1). It is intended to deny enemy forces the use of his electronic equipment, to use his own electronic emissions against him, and to protect ones own electronic equipment against enemy action. EW must then be highly responsive to the action of an enemy and perhaps more importantly to his potential for action (Ref 1:1-2). The need for a particular capability, however, only becomes apparent when the existence of a threat has been established or postulated. It is my own opinion that the development of EW systems is deficient to some degree in the ability to respond. Funding limitations generally inhibit development from proceeding beyond the conceptual phase until a firm threat has been established. Thus it is possible for an enemy to deploy a carefully concealed technique to which we would have no countermeasure. Flexibility is needed in EW systems to meet the potentially diverse spectrum of threats.

A cheap method of determining the efficacy of EW systems against postulated, but unverified threats is necessary, since a usual constraint on development is funding. In this way hardware development, when it became necessary, could proceed with confidence and rapidity. Computer simulation can provide a cheap and flexible, in-house analysis tool for Air Force research and development organizations.

Analysis of the Problem

Assumptions. Two major assumptions are made in the development of this thesis, to simplify the work. They are

not central to the main purpose of developing a tool for the analysis of ECM/ECCM and radar performance:

1) Doctor Berrie's development of the performance of a post-detection integration radar in the presence of synchronized pseudo-random noise is essentially correct. The experiment which will be run to test the effectiveness of SPRNJ against a DICKE-FIX radar receiver, will be designed in accordance with the procedure he outlines.

2) The RADSIM computer simulation is correct in its signal transfer algorithms and radar modular transforms. Errors in these functions, as they apply to the computer to be used, will be corrected within the context of the original design. The radar model algorithms are relatively easy to change due to its modular structure, and in fact are specifically intended for modification as a user requires (Ref 3: 4-3).

Approach to the Solution. The computer simulation to be used in this study was developed under a Rome Air Development Center (RADC) contract for use on a Honeywell 6180 Computer using the General Comprehensive Operating System (GECOS) and FORTRAN IV. It will be converted to the CDC 6600/CYBER74 Computer using SCOPE 3.4 and FORTRAN Extended.

Upon completion of the necessary recoding and operational debugging, a series of test cases will be run to insure that the operation of the simulation, duplicates the same set of cases as run on the Honeywell 6180 Computer. Then an experiment to simulate SPRNJ against a simple search

radar will be designed and executed to confirm the results of Doctor Berrie's theory as demonstrated on the analog computer. An ECCM device (DICKE-FIX) will be added and its performance analyzed. A receiver operating characteristic curve for the radar will be developed for the two cases: with and without the ECCM device.

II. The Theory of Pseudo-Random Noise Jamming

Doctor Berrie's dissertation, identified as ASD TR-74-23 (Ref 2), "The Effect of Pseudo-Random Noise on Radar System Performance" provides a very readable and comprehensive discussion of the theory behind the generation of pseudo-random noise and its use as a radar jamming waveform. This section will summarize the theory presented by Doctor Berrie, and describe some of his results as they relate to this investigation.

Pseudo-Random Binary Sequences

Binary sequences are sequences which are two valued, usually one and zero. A sequence may or may not be periodic, i.e., after some number of values the sequence begins to repeat. A truly random sequence can never be periodic, however, the period of a periodic sequence could be so long that over reasonable observation intervals it would appear to be random. If a periodic sequence shares certain properties of truly random sequences it is termed pseudo-random. The required properties are:

1) The number of ones equals the number of zeros, plus or minus one.
2) $(\frac{1}{2})^n$ of the total number of runs (consecutive elements of the sequence having the same

value) have length n.

3) The auto correlation function of the sequence $C(\tau)$ is two valued and has a value $C(0)$ when $\tau=0$ or an interger multiple (k) of the period (T) and some other value, $C(\tau)$ when $\tau \neq 0$ or kT (Ref 4:280).

The form of the function which generates a periodic binary sequence determines whether or not it is pseudo-random. A function which produces a maximal-length, linear, periodic binary sequence will form a pseudo-random sequence (Ref 2:18).

Generation of Pseudo-Random Sequences

In order to meet the requirements for generation of a linear pseudo-random sequence the expression for the recurrence relationship which describes the sequence must be linear and of the form:

$$a_n = \sum_{i=1}^{r} C_i \, a_{n-i} \qquad (2\text{-}1)$$

a_n = the n^{th} term of the sequence (1 or zero)

C_i = a binary coefficient (1 or zero) of the $n-i^{th}$ term.

a_{n-i} = the preceeding term of the sequence

r = the number of initial terms in the sequence.

The summation is a modulo two summation where the results of

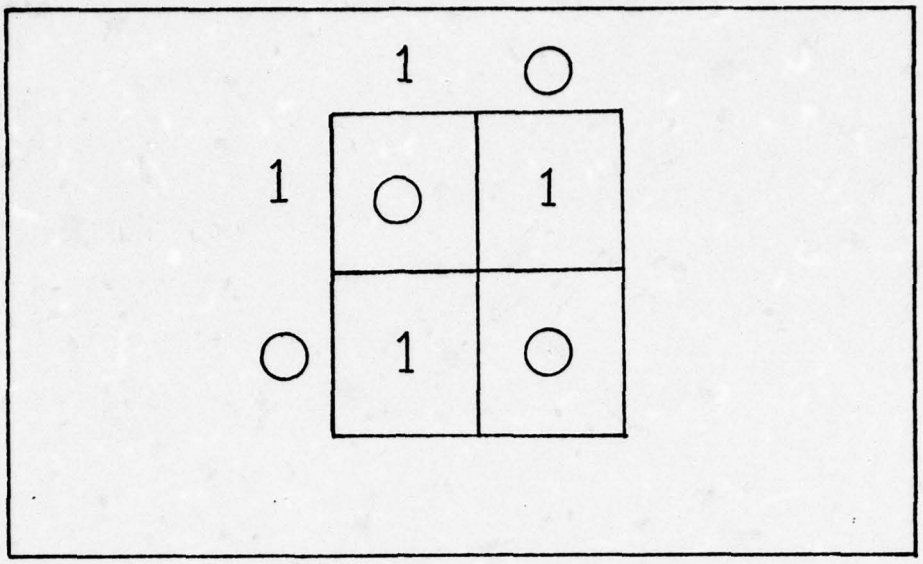

Figure 2. Modulus-Two Addition

the summation are shown in Figure 2. Equations (2-2a) through (2-2d) provide an example of a linear sequence

$$a_5 = a_4C_1+a_3C_2+a_2C_3+a_1C_4 \quad (2\text{-}2a)$$
$$= a_4(1)+a_3(0)+a_2(0)+a_1(1) \quad (2\text{-}2b)$$
$$= (1)(1)+(1)(0)+(0)(0)+(1)(1) \quad (2\text{-}2c)$$
$$= 0 \quad (2\text{-}2d)$$

satisfying Equation (2-1) with four initial terms. The full sequence will have 2^r-1 terms, in this case 15, and would describe all possible states of an r -bit binary number less the all zero state. The all zero state must be excluded to prevent the sequence generation from stopping. If Equation (2-2a) were:

$$a_5 = a_4C_1+a_3C_2+a_2C_3+a_1C_4 \quad (2\text{-}3)$$
$$= a_4(1)+a_3(0)+a_2(0)+a_1(1)$$

$$=(0)(1)+(0)(0)+(0)(0)+(0)(1)$$

$$=0$$

no further terms could ever be generated.

A generating function for a linear pseudo-random sequence may then be defined as:

$$G(x)=\sum_{n=o}^{\infty} a_n X^n \tag{2-4}$$

where a_n is defined in (2-1). Substituting (2-1) into (2-4) leads to the following expression (Ref 2:18).

$$G(x)=\frac{\sum C_i X^i \sum_{k=1}^{i} a_{-k} X^{-k}}{1-\sum_{i=1}^{r} C_i X_i} \tag{2-5}$$

This may be redefined as the ratio of two polynomials.

$$G(x)=\frac{g(x)}{f(x)} \tag{2-6}$$

The polynomial f(x) is the characteristic polynomial of G(x).

$$f(x)=1-\sum_{i=1}^{r} C_i X^i \tag{2-7}$$

$$=1+\sum_{i=1}^{r} C_i X^i$$

If f(x) is a primitive (does not divide modulo two into X^k+1 for values of K less than 2^r-1) and irreducible (cannot be factored into two terms of lower degree) it will produce a maximal length, linear, pseudo-random binary sequence.

ENAD TM-74-01 (Ref 5) also produced by Berrie contains a tabulation of primitive-irreducible polynomials sorted by the number of non-zero coefficients. This tabulation will be later used in developing a shift register to produce pseudo-random noise in Section IV.

Generation of Pseudo-Random Noise with Shift Registers

Equation (2-1) can be easily implemented in a shift register. Figure 3 shows an implementation of Equation (2-1) for r=4. Given some non-zero initial state each stage of the shift register is shifted to the right upon a clock pulse and a_n is shifted into the left most stage. The contents of stages with non-zero C_i are modulo two summed to form a new a_n. The sequence may be obtained one-bit-at-a-time from the a_{n-4} stage or r sequential bits of the sequence obtained at one time from the r registers stages (Ref 2:31). If the C_i's are determined by the non-zero terms of a primitive irreducible polynomial, the sequence generated will be a pseudo-random sequence of length 15.

If the all zero state could occur, the content of each stage could be considered an independent binary random variable, and the sum of all the stages would also be a random variable.

$$Z=\sum_{i=1}^{r} a_i \qquad (2\text{-}8)$$

Z would assume values from zero to r with a probability defined by the binomial distribution (Ref 2:32).

$$P(Z=k)=\binom{r}{k}p^k q^{r-k} \qquad (2\text{-}9)$$

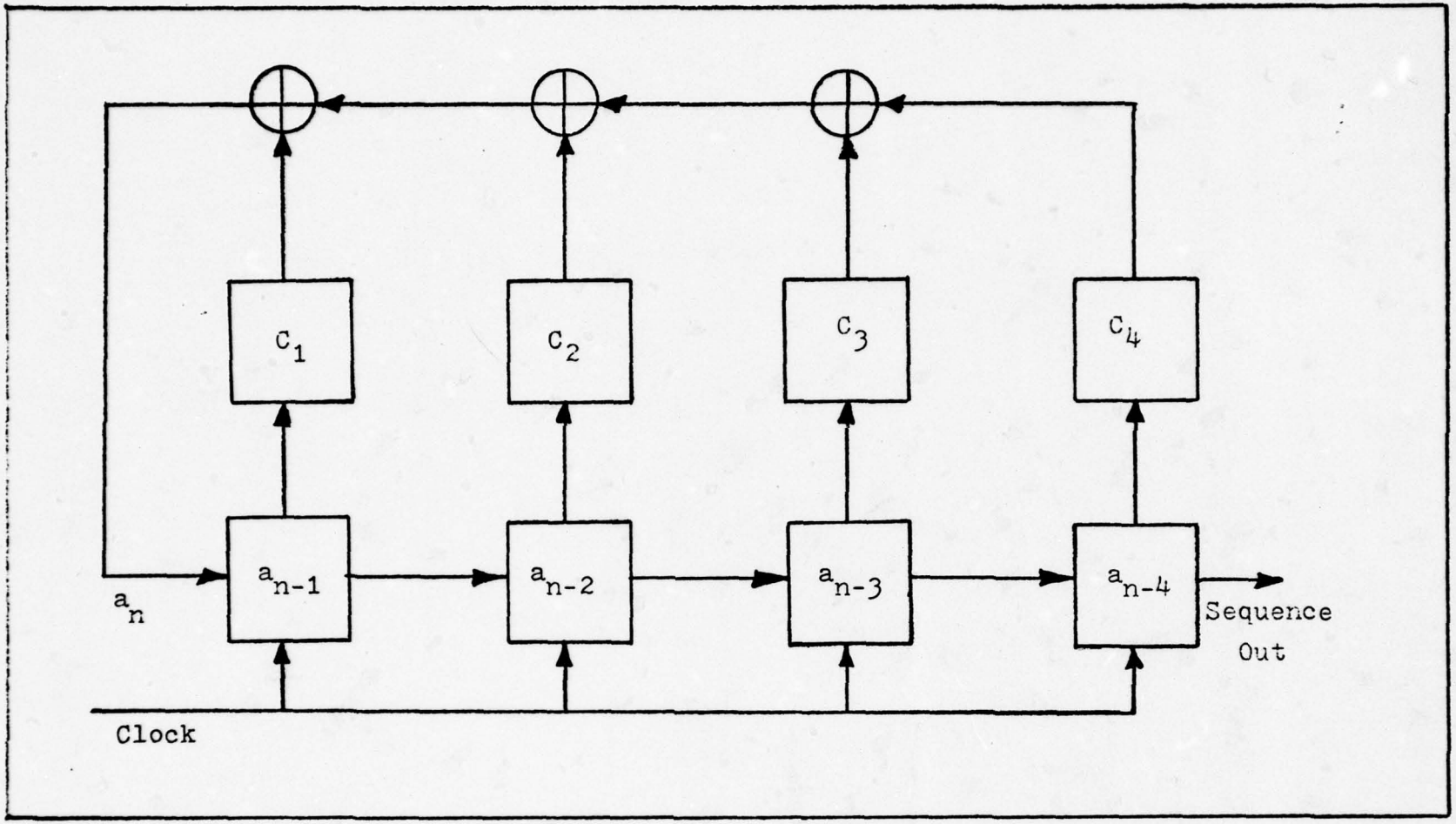

Figure 3. Shift Register Implementation of Linear Recurrence Relationship

When $p=q=\frac{1}{2}$ Equation (2-9) becomes

$$p(Z=k)=\binom{r}{k}\left(\tfrac{1}{2}\right)^{r} \tag{2-10}$$

Papoulis has shown (Ref 6:67) that for large r (r>>4), that 2-10 is asymptotically equal to the Gaussian distribution.

$$P(Z=k)\approx\sqrt{\frac{2}{\pi r}}\exp[-2(k-r/2)^2/r] \tag{2-11}$$

with a mean $\mu=r/2$ and variance $\sigma^2=r/4$. This is not strictly true for the shift register of Figure 3 since the all zero state cannot occur, but for sufficiently large r this will not significantly alter the result (Ref 6:67), and the distribution remains essentially Gaussian.

The Power Density Spectrum of Pseudo-Random Noise

By Papoulis (Ref 6:341) the auto correlation function of a random binary transmission, Figure 4a, shown in Figure 4b is a triangle and its power spectrum is defined by (2-12) and depicted in Figure 4c.

$$S(\omega)=\frac{C(o)4\sin^2(\omega T/2)}{T\omega^2} \tag{2-12}$$

The pseudo-random binary sequence is periodic, however, and its spectrum will be composed of discrete spectral lines whose number will be determined by the sequence length. This is shown in Figure 4d. The expression for the power spectrum of the pseudo-random sequence is:

$$S_f(\omega)=2\pi\left[\frac{\delta(\omega)}{N^2}+\frac{N+1}{N^2}\sum_{\substack{n=-\infty\\ n\neq 0}}^{\infty}\left(\frac{\sin n\pi/N}{n\pi/N}\right)^2\delta\left(\omega-n\frac{2\pi}{L}\right)\right] \tag{2-13}$$

N = the number of bits in the sequence

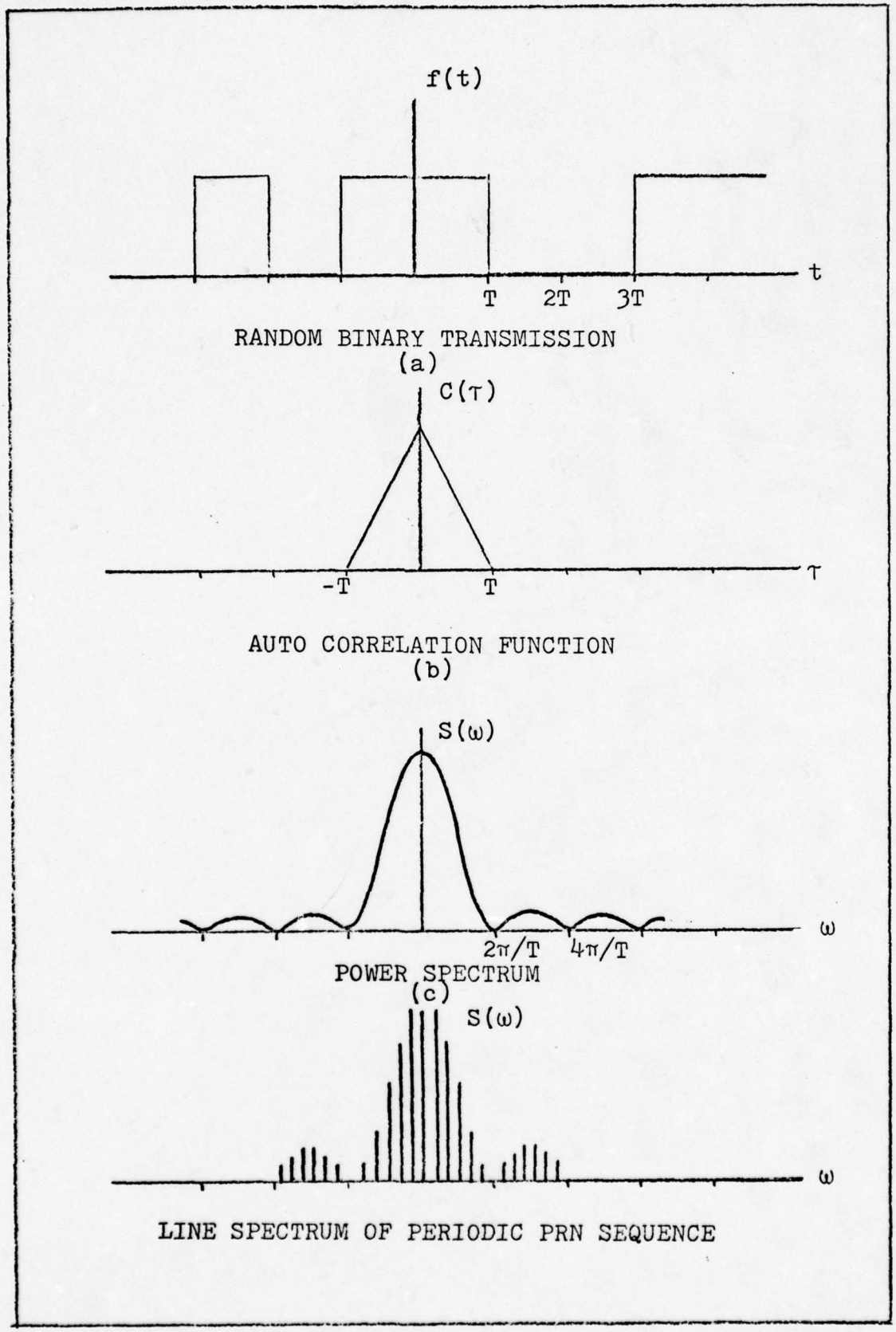

Figure 4. Random Binary Transmission, Autocorrelation Function and Power Spectrum

The zeros of this spectrum will occur when n/N is an integer multiple of the clock frequency.

It has been shown (Ref 2:33-35) that the summation of the stages of the register is equivalent to low pass filtering of the sequence. This results in a decrease in the width of the spectrum main lobe by a factor of 1/r where r is, as before, the number of stages in the shift register. The spectrum now appears as in Figure 5.

Generation of PRN Signal for Jamming

The spectrum of the shift register pseudo-random noise generator contains elements which range in frequency from zero to the clock frequency divided by r. To be useful for jamming this spectrum must be translated to radar frequencies. A method of doing this would be to use the sum of the registers to modulate a sinusoidal carrier. In this study, double sideband (DSB) modulation will be used and Equation (2-14) will be the expression of the jamming signal.

$$J(t) = Z(t)\cos(\omega_c t + \phi) \qquad (2\text{-}14)$$

$J(t)$ = the jamming signal

Z = the register sum

ω_c = the carrier frequency

ϕ = some phase angle

If this signal is within the radar bandpass some degree of interference will be seen in the radar detection process. Figure 6 shows a block diagram of the jammer, and the transmitted spectrum.

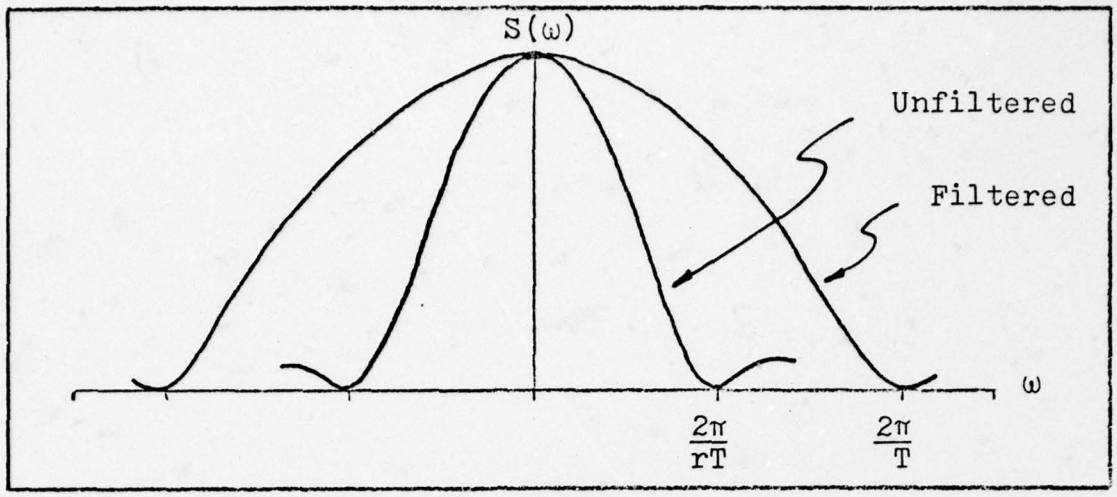

Figure 5. Filtered and Unfiltered Pseudo-Random Sequence Power Spectrum Envelope

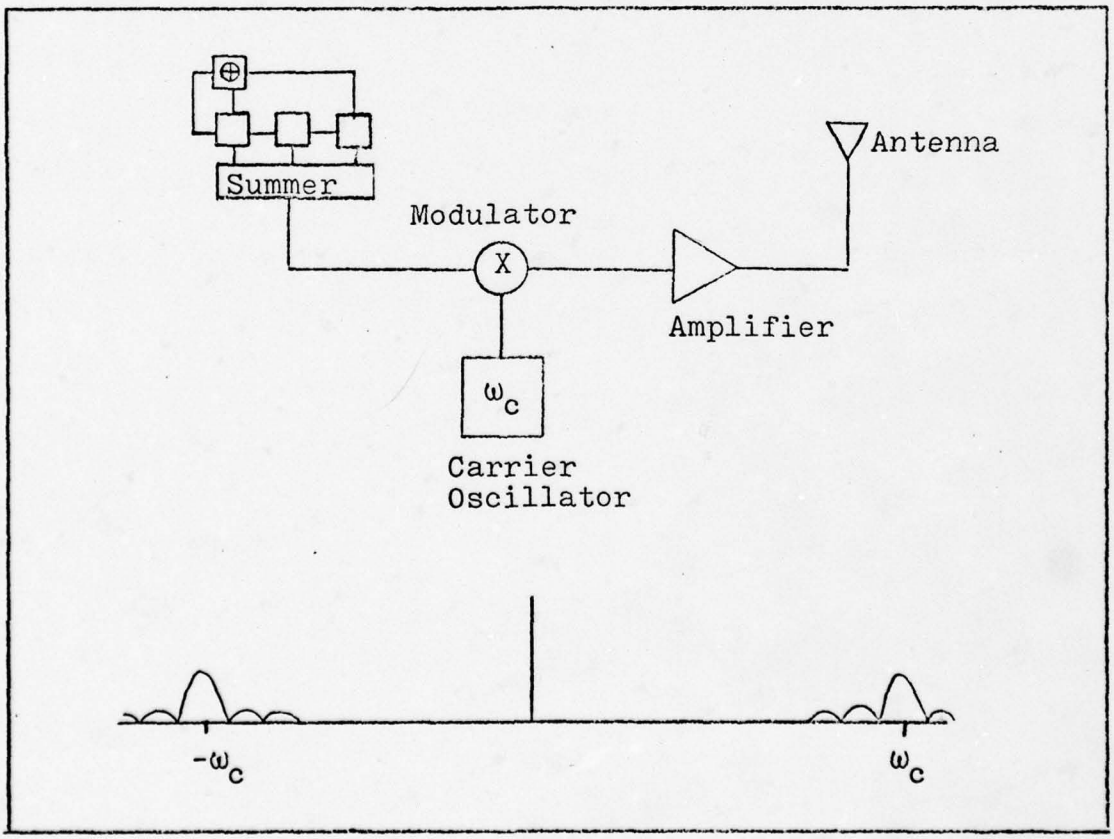

Figure 6. Block Diagram of PRN Jammer and its Spectrum

The Application of Pseudo Random Noise to Radar Jamming

A block diagram of a typical search radar is shown in Figure 7. The transmitter sends out relatively short R-F pulses at specific intervals (typically 200-400 pulses-per-second), controlled by a stable local oscillator. The pulses are reflected from the target, received at the radar antenna and reduced to some convenient intermediate frequency (IF). They are then detected and used to drive some form of display which presents the pulses received on a scale relative to the total round-trip time from transmitter to target and back to the receiver.

The detection process is essentially a binary detection process with two hypotheses (Ref 8:27).

$$H_o: \underline{r}(t)=\underline{n}(t); \quad \text{noise only} \qquad (2\text{-}15)$$
$$H_1: \underline{r}(t)=\underline{n}(t)+s(t); \quad \text{signal + noise}$$

$\underline{r}(t)$ = the received signal

$\underline{n}(t)$ = noise

$s(t)$ = the reflected signal

The intermediate frequency filter is a matched filter in most radars (Ref 7:74) whose impulse response is matched to the form of the transmitted pulse $S(t)$.

$$H(\omega)=S^*(\omega)e^{-j\omega t_o} \qquad (2\text{-}16)$$

$H(\omega)$=filter frequency characteristic

$S^*(\omega)$=signal spectrum complex conjugate

When only noise is considered H_o is the hypothesis and $\underline{r}(t)=\underline{n}(t)$. The signal out of the filter (Figure 7) is $\underline{x}(t)$.

$$\underline{x}(t)=\underline{N}(t)\cos[\omega_o t-\underline{\phi}(t)] \qquad (2\text{-}17)$$

$\underline{N}(t)$ and $\underline{\phi}(t)$ are independent random variables which are normally and uniformly distributed respectively. The sam-

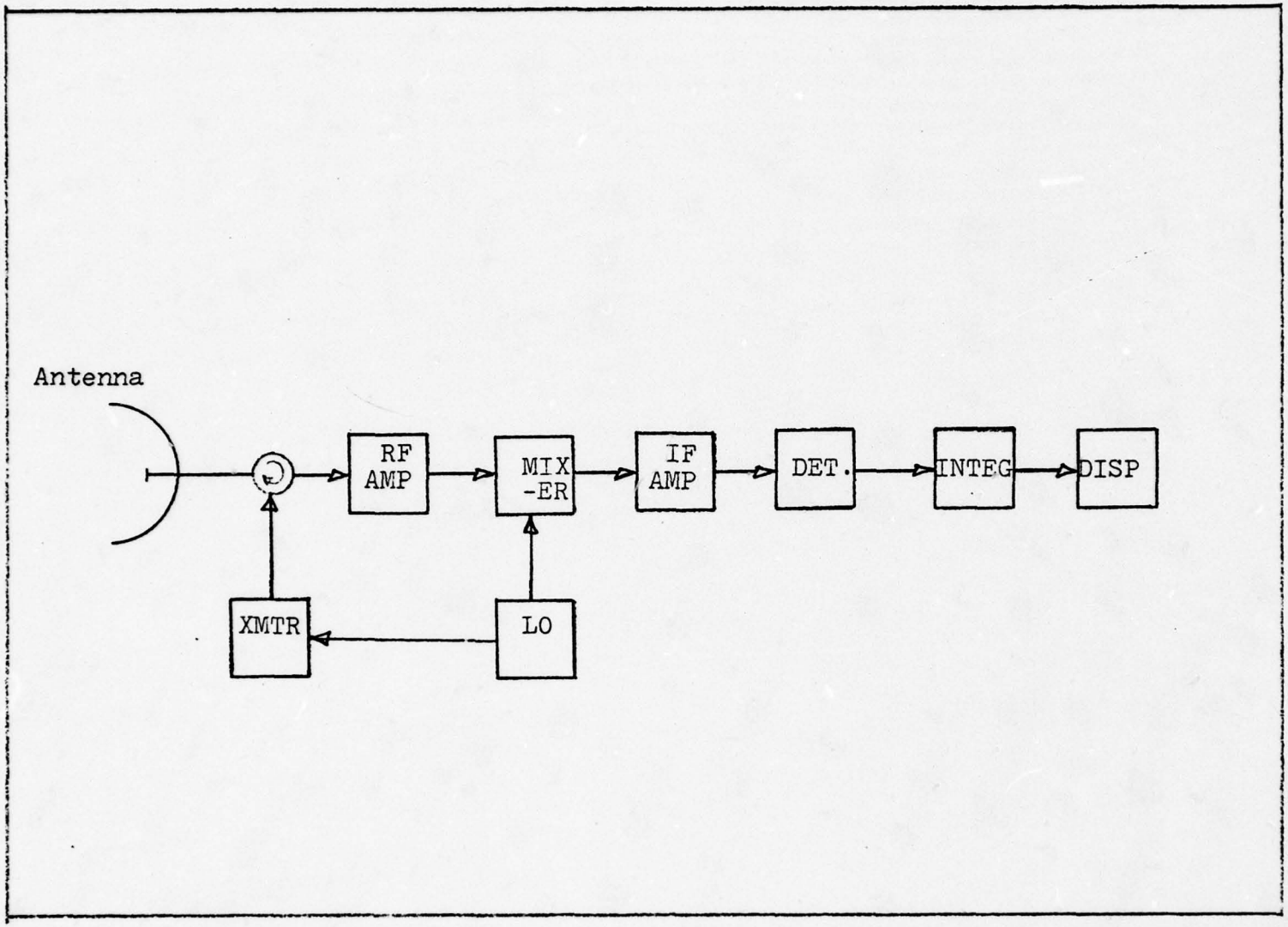

Figure 7. Block Diagram of A Typical Search Radar

ples of the noise are:

$$W(N_i)=\frac{}{\sqrt{2\pi\sigma_N^2}}\exp[-N_i^2/2\sigma_N^2] \qquad (2\text{-}18)$$

with zero mean and variance σ_n^2. If the target signal is present, then H_1 is true.

$$\begin{aligned}\underline{r}(t)&=\underline{N}(t)+S(t)\\&=\underline{N}(t)+A[1+\cos\omega_o t]\\&=(\underline{N}_1+A)\cos\omega_o t+\underline{N}^2\sin\omega_o t\\&=\underline{X}_1(t)\cos\omega_o t+X_2(t)\sin\omega_o t\end{aligned}$$

X_1 and X_2 are statistically independent random variables and:

$$W(X_1)=\frac{1}{\sqrt{2\pi}\sigma_N}\exp[-(X_1-A)^2/2\sigma_N^2] \qquad (2\text{-}19)$$

$$W(X_2)=\frac{1}{\sqrt{2\pi}\sigma_N}\exp[-X_2^2/2\sigma_N^2] \qquad (2\text{-}20)$$

$$W(X_1,X_2)=\frac{1}{2\pi\sigma_N}\exp\left[-\frac{(X_1-A)+X_2^2}{2\sigma_N^2}\right] \qquad (2\text{-}21)$$

Translating 2-21 to polar coordinates by setting $X_1=R\cos\phi$ and $X_2=R\sin\phi$ we can integrate with respect to ϕ and normalize with respect to σ_N to obtain the joint probability density function of the IF filter output.

$$W(v)=ve^{-(v^2+a^2)}I_o(av) \qquad (2\text{-}22)$$

$a=A/\sigma_N$

$v=R/\sigma_N$

$I_o(av)$=zero order modified Bessel Function.

Since a is the amplitude of the signal, s(t), for the noise only case, a in Equation (2-22), will be zero making the density Rayleigh. For a signal present, a will have some non-zero value and the output will be a Generalized Rayleigh (Rician) distribution (Ref 2:177). Figure 8 shows a plot of

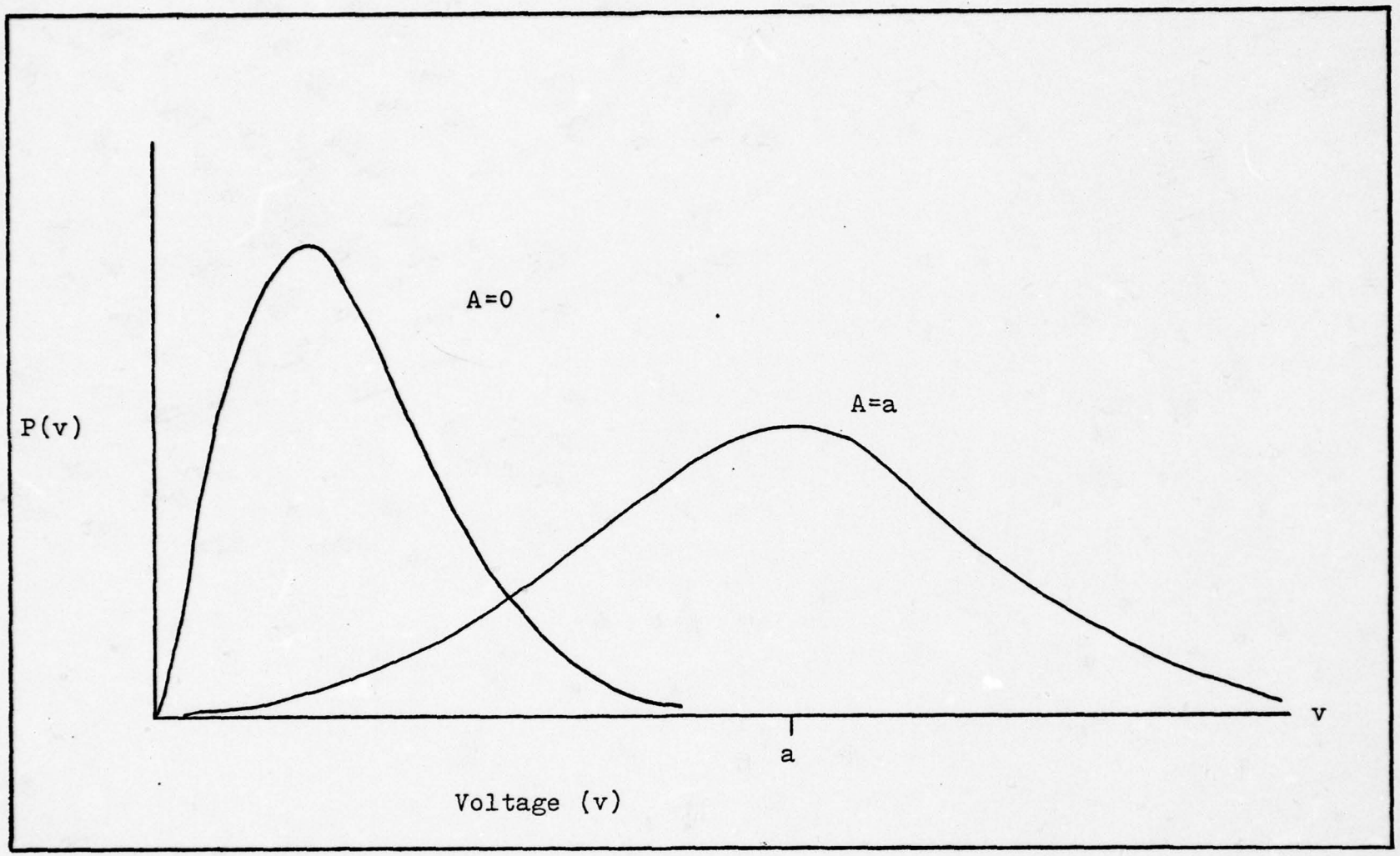

Figure 8. Plot of Equation 2-22 for Two Values of A. A = 0, and A = a.

Equation (2-22) for the noise only and a signal plus noise case.

Probability of detection is defined as the probability that the signal plus noise voltage will exceed some threshold voltage γ, and probability of false alarm is defined as the probability that the noise alone will exceed the same threshold. These probabilities are shown pictorially in Figure 9. Their expressions are shown in Equations (2-23) and (2-24).

$$P_d = \int_{\gamma}^{\infty} v e^{\frac{-v^2+a^2}{2}} I_o(av)\,dv \qquad (2\text{-}23)$$

$$P_{fa} = \int_{\gamma}^{\infty} v e^{-v^2/2}\,dv \qquad (2\text{-}24)$$

Pulse Integration

Some radars use pulse integration to improve the probability of detection. The pulse integrator shown in Figure 10 adds several pulses after detection and prior to the thresholding of Equations (2-23) and (2-24). The impulse response of the integrator is:

$$h(t) = \sum_{k-o}^{k-1} \delta(t-kT) \qquad (2\text{-}25)$$

K=number of pulses to be integrated

T=the pulse repitition interval

thus $d(t)=y(t)*h(t)$ and,

$$d(t) = \sum_{k=0}^{K-1} y(t)(t-kT) \qquad (2\text{-}26)$$

If y(t) is periodic:

$$d(t)=Ky(t) \qquad (2\text{-}27)$$

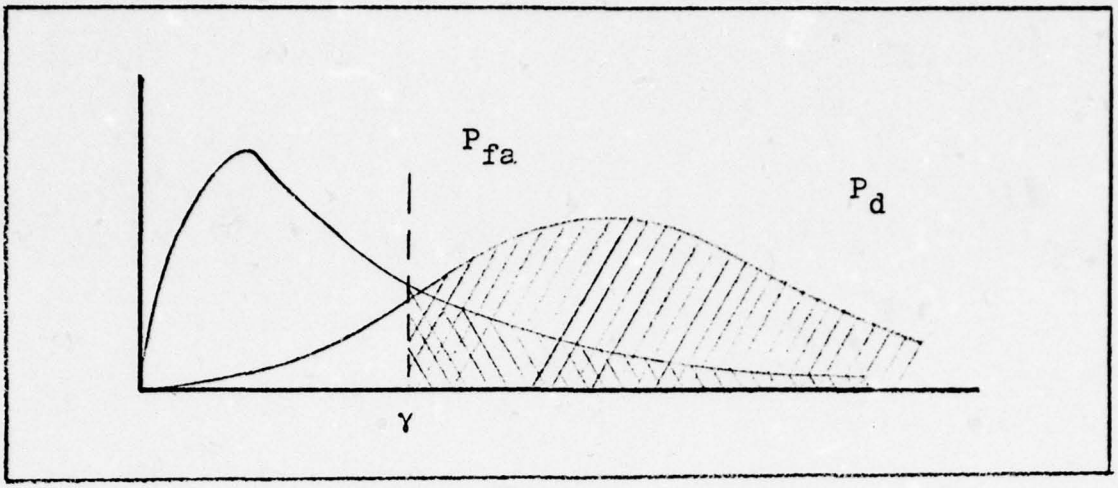

Figure 9. Pictorial Representation of P_d, P_{fa}.

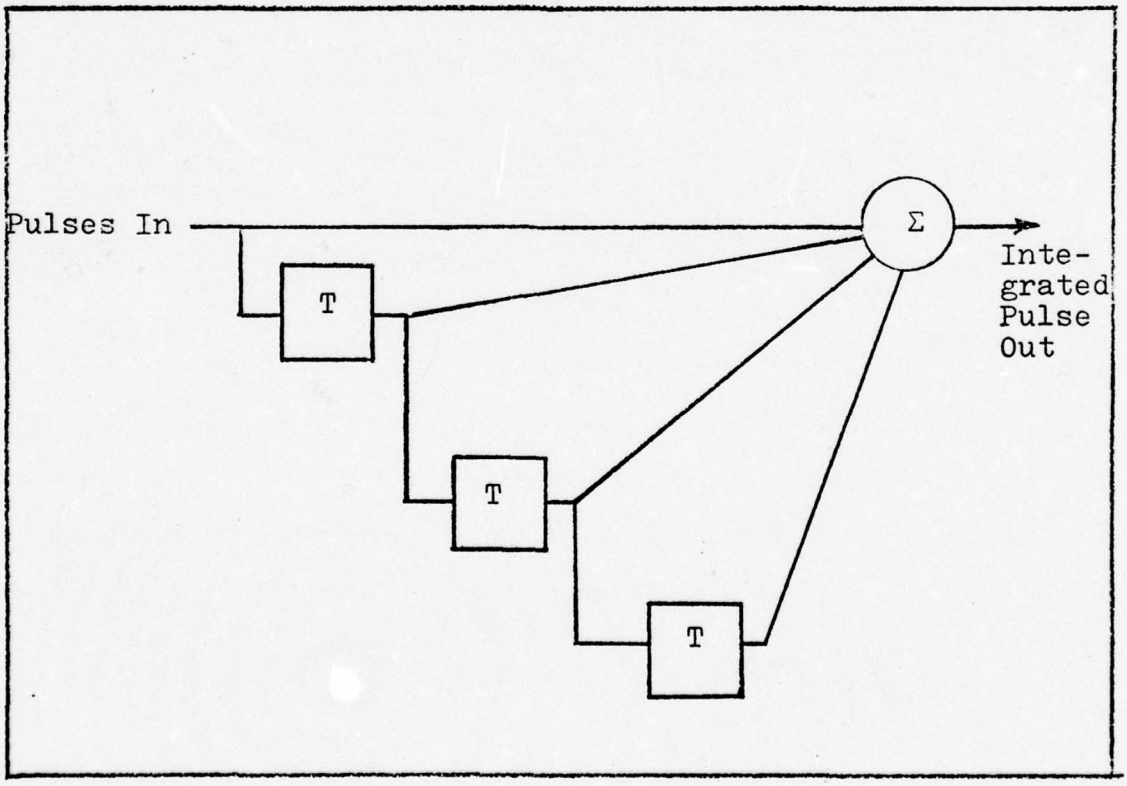

Figure 10. Block Diagram of a Pulse Integrator

When y(t) is a random variable, the sum of the K additions will also be a random variable, normally distributed with mean μ_r and variance σ_r^2.

$$\mu_r=\sum_{i=1}^{k}\mu_i=K\sqrt{\frac{\pi}{2}}\sigma_N \tag{2-28}$$

$$\sigma^2_r=K(2-\frac{\pi}{2})\sigma_N^2 \tag{2-29}$$

μ_i=mean of the input signal

σ_N^2=variance of the input noise

The distributions for the envelope of the noise only and the signal plus noise are respectively normalized to the input noise variance:

$$P_n(v)=\frac{1}{\sqrt{2\pi K(2-\pi/2)}}\exp[-(v-K\sqrt{\frac{\pi}{2}})^2/2k(2-\pi/2)] \tag{2-30}$$

and

$$P_{s+n}(v)\frac{1}{\sqrt{2\pi(2-\pi/2)}}\frac{\sigma_R}{\sigma_N}\exp[-(v-K\mu_r/\sigma_N)^2/2K\sigma_R^2/\sigma_N^2] \tag{2-31}$$

The probability of detection and false alarm may be found by integrating Equations (2-30) and (2-31) from the threshold to infinity as in Equations (2-23) and (2-24) and shown in Figure 9.

Figure 11 shows the result of such integration performed by Berrie for eight pulses integrated at several signal-to-noise ratios.

When synchronized pseudo-random noise is present it is a periodic signal. This by Equation (2-27) its form will be the same at the output of the integrator as at the input.

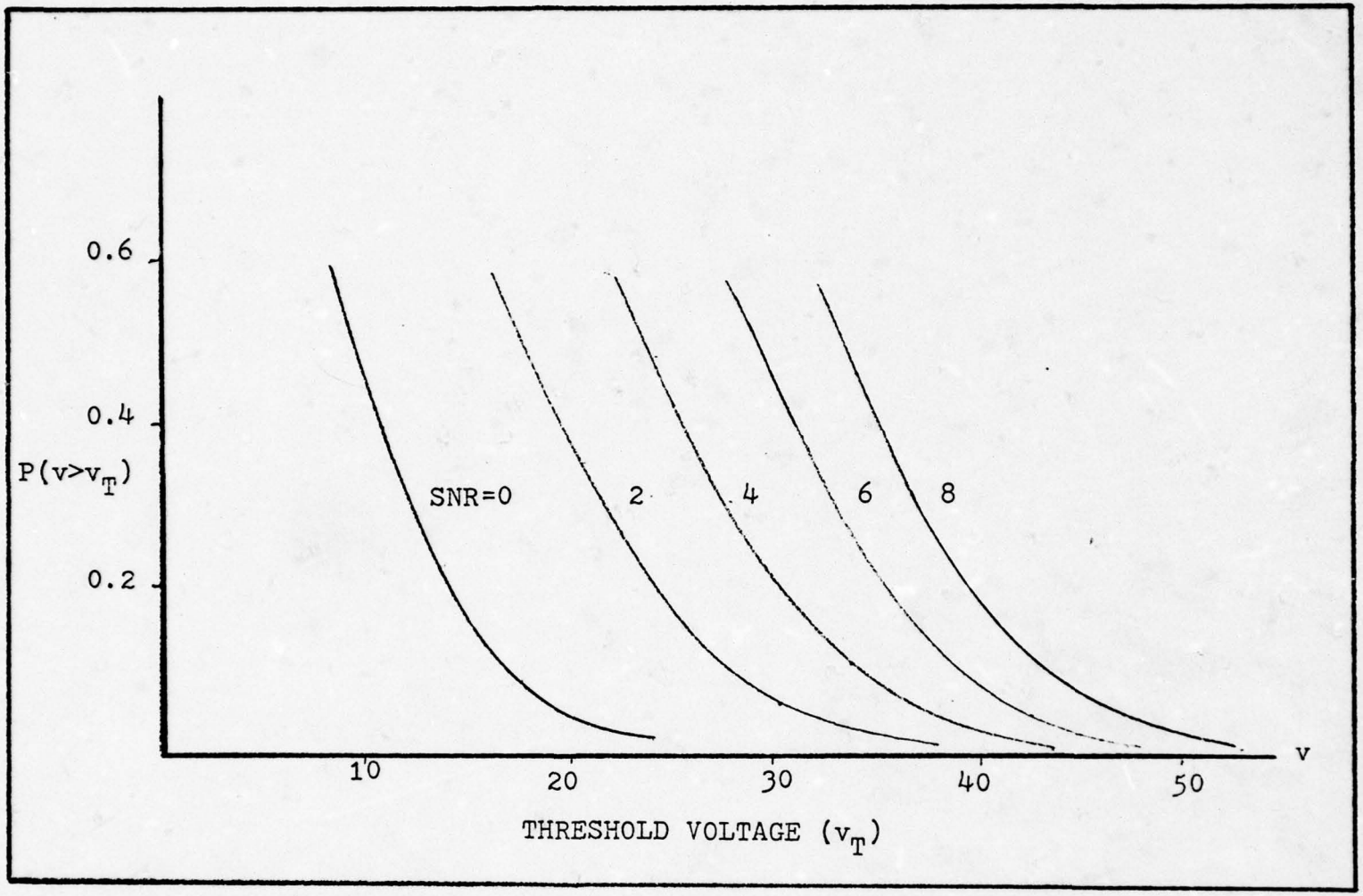

Figure 11. Probability of Voltage Exceeding Threshold (P_d) for Eight Integrated Pulses at Five Signal to Noise Ratios.

If $P_{s+n}(v)=ve^{-\frac{v^2+a^2}{2}} I_o(av)$ then: (2-32)

$$P_{s+n}(kv)=\frac{kv}{k^2} e^{-\frac{v^2+(ak)^2}{2k^2}} I_o\left(\frac{av}{k}\right) \quad (2-33)$$

When P_d and P_{fa} are calculated for the integrated signal, no improvement over the pre-integrated case is found (Ref 2:180).

Results of Berrie's Experiment

Berrie analyzed the performance of synchronized pseudo-random noise against a typical search radar. He used an analog computer model of the radar scaled to audio frequencies for the analysis. The results of his experiment showed that the probability of detection was reduced in a post detection integrator when this form of jamming was present. Table I shows the results of his experiment, for thermal random noise (TRN) and SPRN.

Table I
Probability of Detection For P_{fa}=0.1
at Integrator Input and Output

SNR	P_d Integrator Input SPRN/TRN	P_d Integrator Output SPRN/TRN
2	.45/.31	.30/.64
4	.70/.41	.40/.74
6	.75/.52	.50/.80
8	.85/.65	.60/.84
10	.92/.71	.70/.86

As would be expected the improvement, or rather degradation in detection probability, is lessened with increasing SNR,

but at low SNR the improvement is quite dramatic.

This chapter has described how pseudo-random sequences may be recognized and generated using primitive irreducible polynomials. A shift register implementation of a pseudo-random sequence generator was shown and the characteristics of the output of a noise jammer based on this sequences generator depicted. The basic principles of radar detection were very briefly outlined and the way in which synchronized pseudo-random noise would affect a post-detection integrator explained. Berrie's result of an experiment to evaluate the effect of synchronized-pseudo-random noise based jamming was summarized. This treatment was by no means exhaustive. Most of the detail is treated in ASD TR-74-23, and a reader interested in the derivations should refer to that document.

III. The Radar Simulation

One of the objectives of this study is to provide to AFIT and ASD a computer program for the analysis of radar/communications hardware and waveforms. This objective is met by converting an existing program, developed by the Rome Air Development Center for use on a Honeywell Information System 635/6180 computer to the ASD CDC 6600/CYBER74 computer. This section will describe the development of the RADSIM simulation program, and explain the major changes required to convert it to the CDC computer. It will also briefly explain how to structure a problem and prepare data cards. Complete program documentation is provided in the four volumes of RADC TR-76-186, and in the source code as altered to run on the CDC system. While the simulator main programs execute correctly, some of the subroutines remain unverified for CDC use.

Background of RADSIM Development

The RADSIM computer program was developed by the Convair Aerospace Division of General Dynamics for Rome Air Development Center under Contract F-30602-73-C-0380. It is intended to provide RADC with a simulation which can be used to predict radar system performance in many different environments. A major feature of RADSIM is the ability to include real world data for simulation validation (Ref 3:xxi).

With these features, radar engineers who are not experienced simulation designers can easily model systems and perform tradeoff studies without commitment to expensive hardware prototypes.

The approach chosen for the development of this simulation is to model the various components of a radar system as separate modules. The modular components are then linked as necessary with a driving program to simulate the desired system. Component models are based on either mathematical expressions or measured data (Ref 3:2-2). RADSIM is coded in FORTRAN IV and designed so that an engineer who thoroughly understands radar system analysis, but is not an experienced FORTRAN programmer can use it with a minimum of assistance.

Currently work is being done to extend the simulation capability of ECM/ECCM performance studies and to provide for interactive operation. The modelling of Communications problems has also been considered. In 1975 the Naval Surface Weapon Center (NSWC) began a project to translate the program for use on a CDC 6600 computer at the Dahlgren Laboratory, but was forced to terminate their effort due to other priorities. When RADSIM was selected for this study, NSWC provided a partially converted source program for use on the ASD computer system.

RADSIM Structure

The RADSIM program design approaches radar modelling by considering the radar system as a collection of subsystems divided into functional elements such as amplifiers,

filters, and analog to digital converters as shown in Figure 12. Each of the elements can be modeled by specifying its transfer function as either a mathematical expression or as measured or derived data for table look up. By linking these functional elements to synthesize radar subsystems, such as a transmitter, receiver, display, or antenna, and specifying the appropriate parameters of the transfer function, a very flexible and comprehensive radar simulation can be constructed. In RADSIM each functional element has been implemented as a module with a distinctive module reference number (MRN). Usually a module is a single subroutine, for instance MRN 401 references subroutine NONLIN which represents a zero-memory nonlinear device as shown in Figure 13. The transfer function for this module is defined by specifying the corners of the desired non-linear function and linear interpolation is used between those points.

Data for signal processing is contained in arrays stored in common areas for access by all modules. All signal data is processed in blocks from these arrays to reduce CPU overhead and to allow snapshots of the radar signal states to be observed at any point in the simulation. Figure 14 shows how several modules may be linked to simulate a simple radar receiver and the data extracted from the system at several points.

There are two main programs in the RADSIM simulation. The first processes the input data which describe the radar system elements and signals and passes them to the simulation

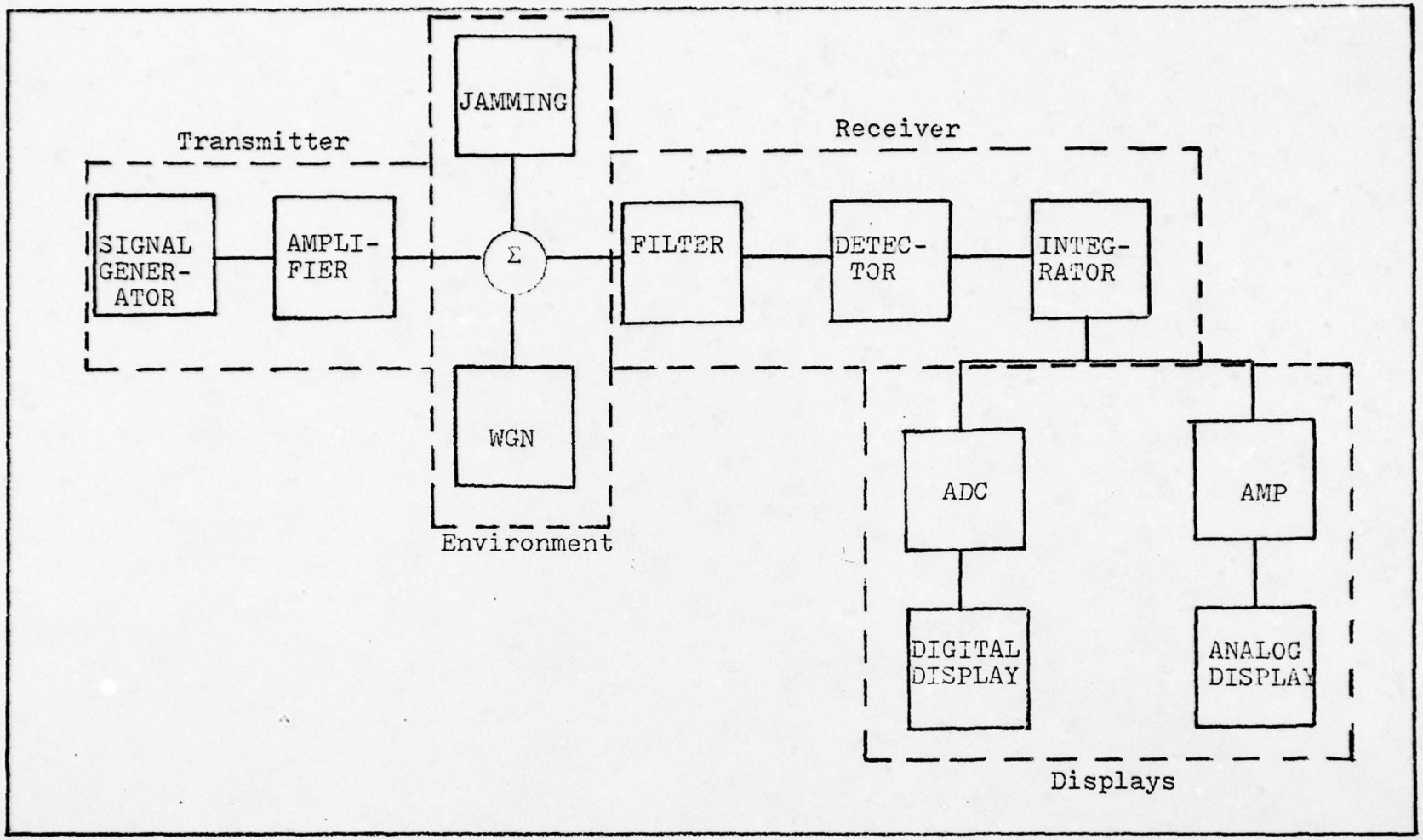

Figure 12. Radar Subsystem and Functional Elements

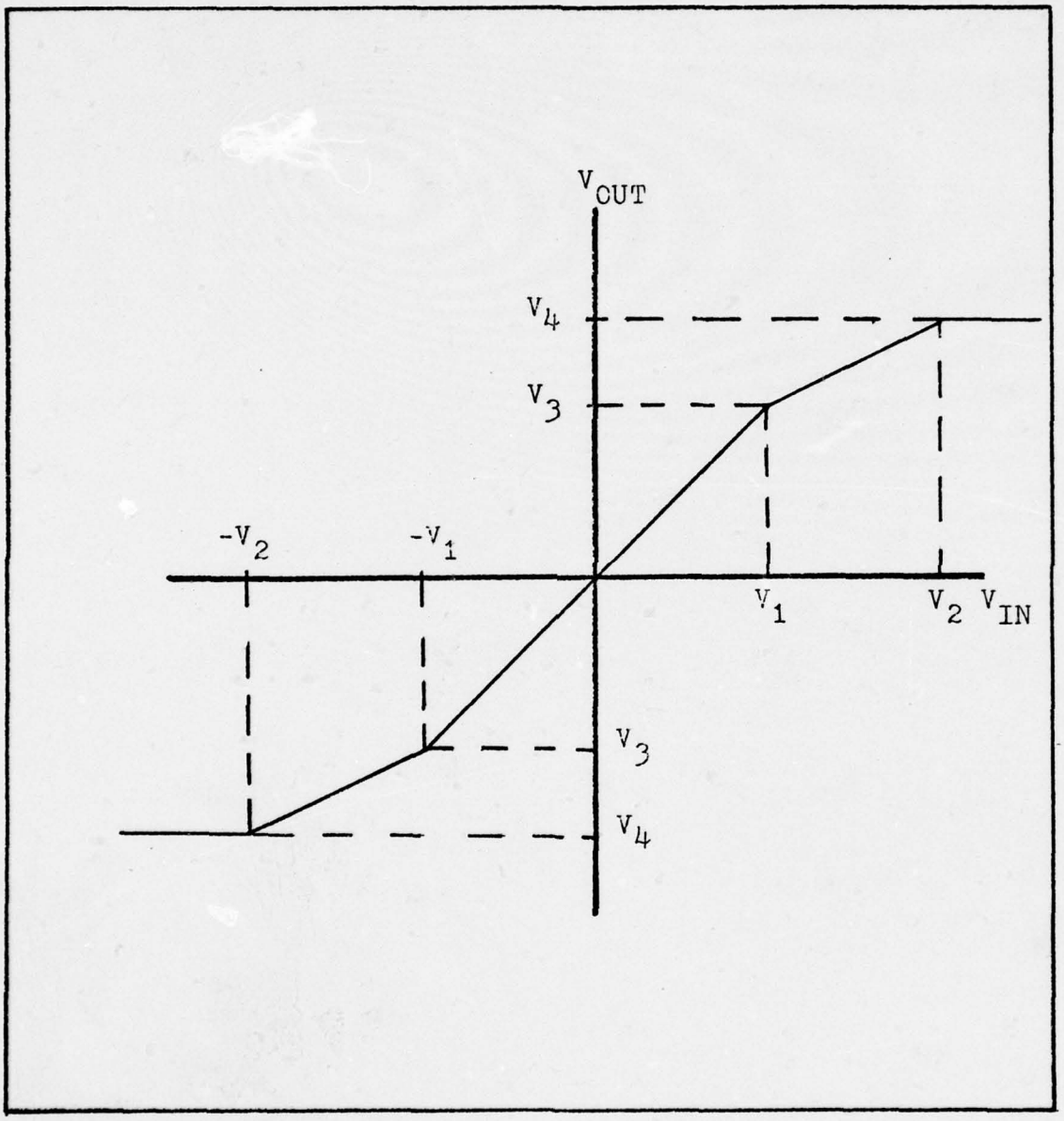

Figure 13. Zero Memory Non-Linear Device

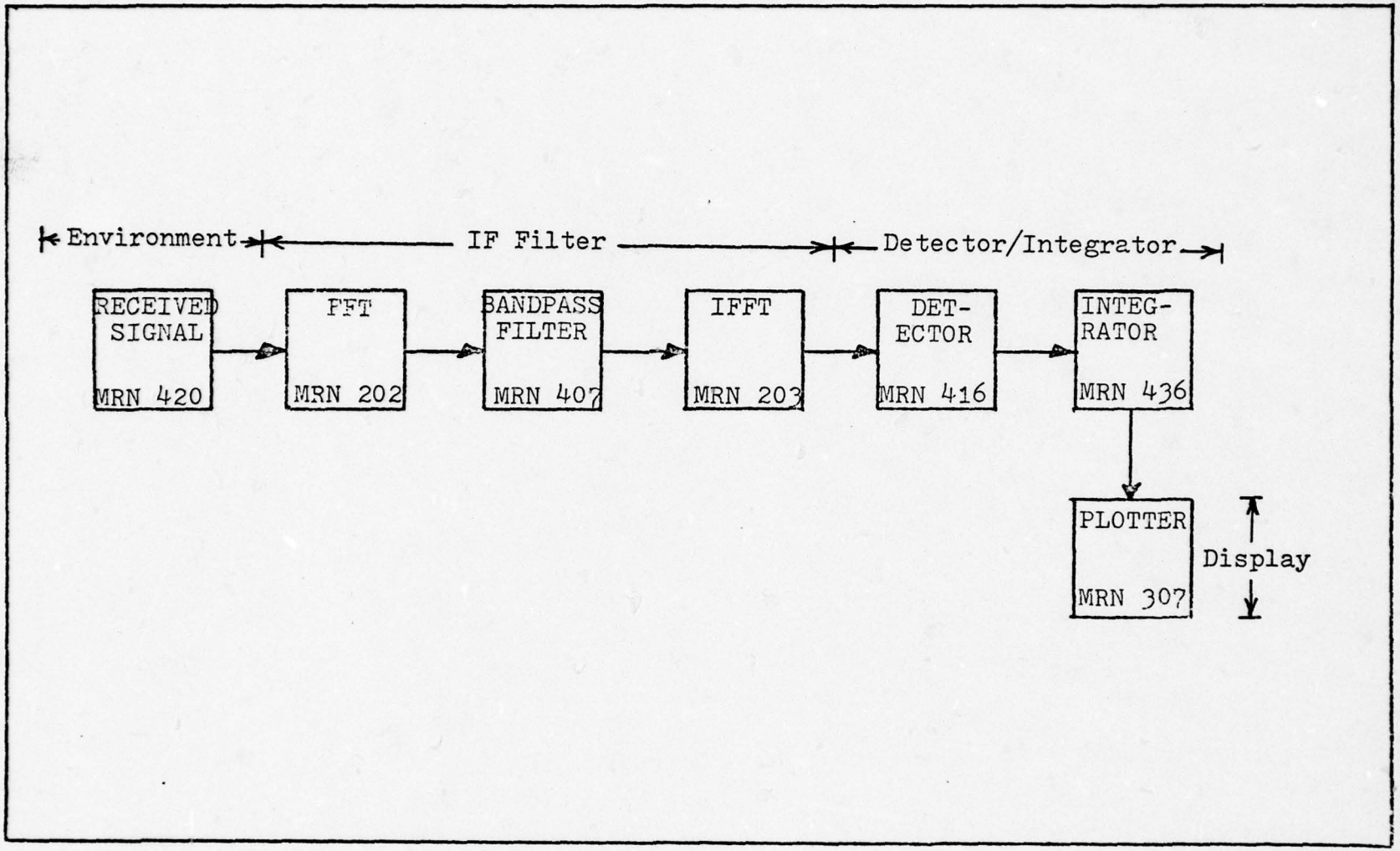

Figure 14. Modules Linked for Receiver Model

driver, the second program. These programs are named RADSIM and RADSIM2 respectively, but are stored as LOADR and SIMEX. (Figure 15 shows the flow of data through the simulation activity).

Mathematical Background of RADSIM

Waveforms can be expressed in real systems as functions of time, S(t), or frequency, S(f).

where:

$$S(f)=\int_{-\infty}^{\infty} S(t)e^{-j^2\pi ft}\,dt \qquad (3\text{-}1)$$

a sampled waveform of S(t) can be defined as:

$$S_*(t)=S(t)T\sum_{n=-\infty}^{n=\infty}\delta(t-nT) \qquad (3\text{-}2)$$

where T = the sample interval. Then the discrete representation of S(t) over some time interval $-NT\leq t\leq NT$ will be

$$S_n=TS(nT) \qquad (3\text{-}3)$$

The Fourier transform of this sampled function $S_*(t)$ is $S_*(f)$, and the discrete frequency samples will be

$$S_k=\sum_{n=N}^{N} TS(nT)e^{-j2\pi nk\Omega t}$$

$$\Omega=\frac{2^{-N2}}{T} \qquad (3\text{-}4)$$

$S(k\Omega)$ is defined as the Discrete Fourier Transform (DFT) of $S(nT)$ and $H(k\Omega)$ as the DFT of $h(nT)$. Discrete convolution can be performed on these two elements as shown in Equation 3-5.

$$H(k\Omega)S(k\Omega)=DFT\left[\sum_{n=-N}^{N} S(nT)h[Mod(N,(M-n))T]\right] \qquad (3\text{-}5)$$

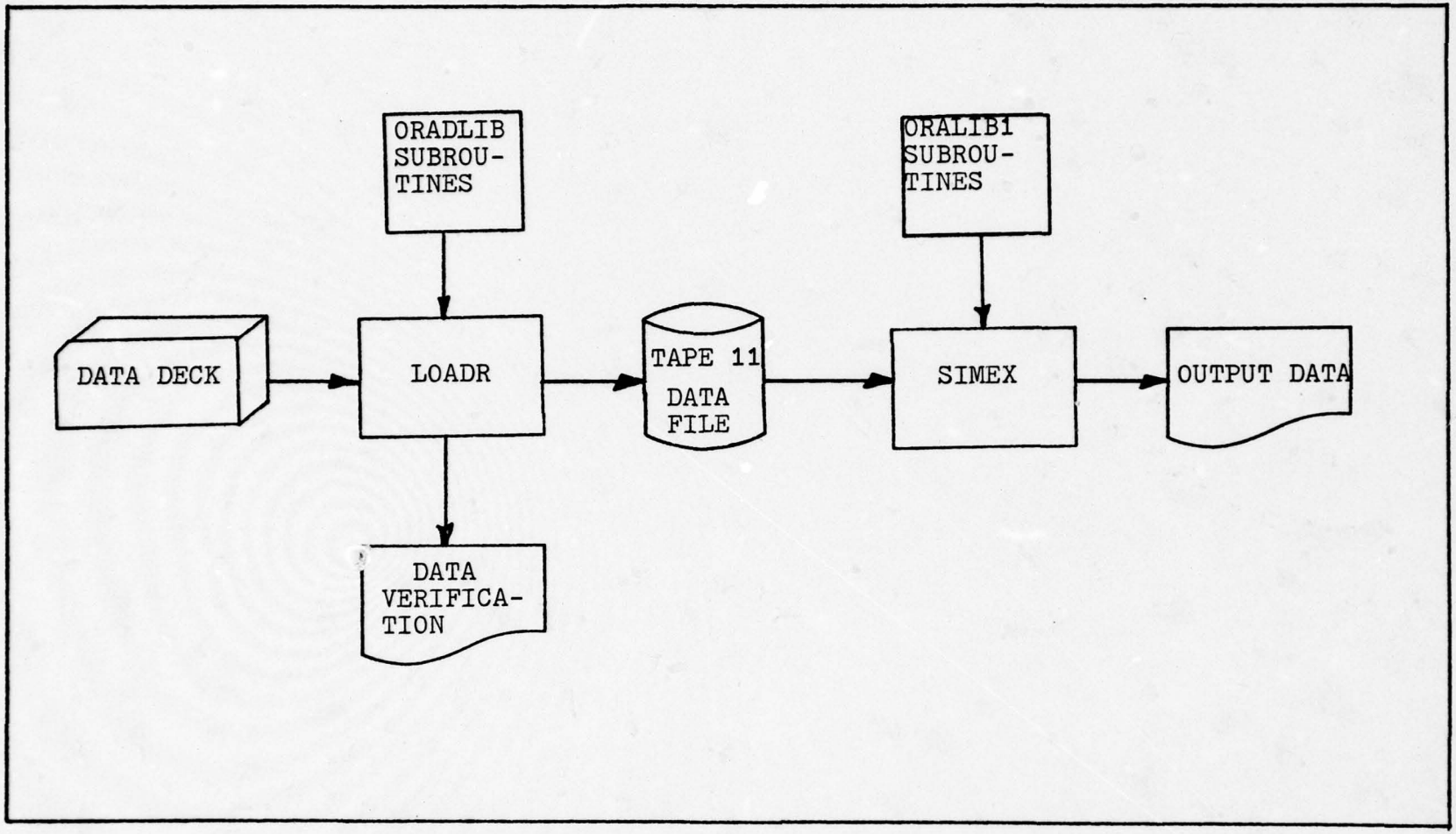

Figure 15. Simplified Data Flow Through Simulation

where MOD(N,(M-n)) is (M-n) Modulo N. M is the lag term of the convolution. This discrete convolution can be used in determining the response of a linear time-invariant system to some signal S(t) (Ref 3:3-32). More details on the representation of specific signal forms and physical systems can be found in Section 3 of RADC TR 76-186. Some tradeoffs were required between sampling rates (T) and signal storage space in the simulation. While higher sampling frequencies and therefore more sample points reduces aliasing and generally leads to more accurate results, it was necessary to keep the array sizes within some reasonable bound. An array size of 8192 (2^{13}) points was chosen. Array sizes can be expanded by allowing overflow into sequential arrays, but some simulation flexibility is lost in the process (Ref 3: 7-25).

Major Changes to RADSIM

An attempt was made to modify the program for the ASD System with changes which would not significantly alter the conceptual integrity of the simulation. It was necessary to keep the changes as small as possible and restrict the scope of their effect to very localized portions of the code. This section describes the changes.

1) The HIS FORTRAN IV calls for access to direct access storage have been changed to use the READMS/ WRITMS functions of FORTRAN Extended. The dimensioned areas KEY (600) in RADSIM1 and RADSIM2 are used to

hold the table of direct access file indexes (Ref 9: I-8-9).

2) Honeywell FORTRAN IV differs from CDC FORTRAN in the use of subroutine entry point arguments. In Honeywell FORTRAN each entry point may have its own list of arguments. In CDC FORTRAN Extended, the entry point assumes the arguments of the parent subroutine. All subroutine arguments and calling arguments have been modified. Where an argument is not to be used a dummy variable (DUM1 or DUM2) is inserted in the call.

3) The Honeywell version of FORTRAN included a function (FLD) for bit manipulation within words. The CDC subroutine STRING from the CDC6600 Library was selected to perform this function (Ref 10:A-14).

4) A function to allow the transfer of data from a real to an integer variable, or vice versa, without bit position rearrangement was required. In Honeywell FORTRAN the intrinsic function BOOL performs this "ignore type" requirement. Such a feature is not available in CDC FORTRAN Extended. It was provided by writing two functions BOOL and IBOOL. They are documented in the source code, and equivalence a location as both a real and integer variable. NSWC changed some of the required function references to perform the function within the module code itself. These changes are fully compatible with BOOL and IBOOL, but could well be replaced with function calls to make the

program structure more consistent.

5) File declarations are made with control cards on the Honeywell system. A PROGRAM statement has been added to RADSIM to reflect CDC FORTRAN conventions.

6) Honeywell uses a 36 bit word. Many FORMAT statements to write data in octal or A format use A6 or 06. Where encountered these have been changed to A10 or 010.

7) The program uses Namelists to read input data. In some cases it is required to input labels for graphical output. Since Hollerith characters are not allowed in CDC FORTRAN Namelists, the characters are entered on data cards following the namelist data. The number of words of Hollerith data in the label is read using the Namelist.

8) A line printer plotting routine was added to aid in examining data.

Simulation Set-up and Use

The first step in a simulation is to decide upon a radar system or subsystem to be simulated and to draw a block diagram of the elements. These elements must be specified in terms of the functional elements available in the RADSIM program. Output modules are then added as desired, and all elements are specified in terms of their module reference number (MRN). Figure 16 shows the radar model of Figure 12 in terms of RADSIM modules. Using the tables of Appendicies B and C of RADCTR-76-186 the required parameters

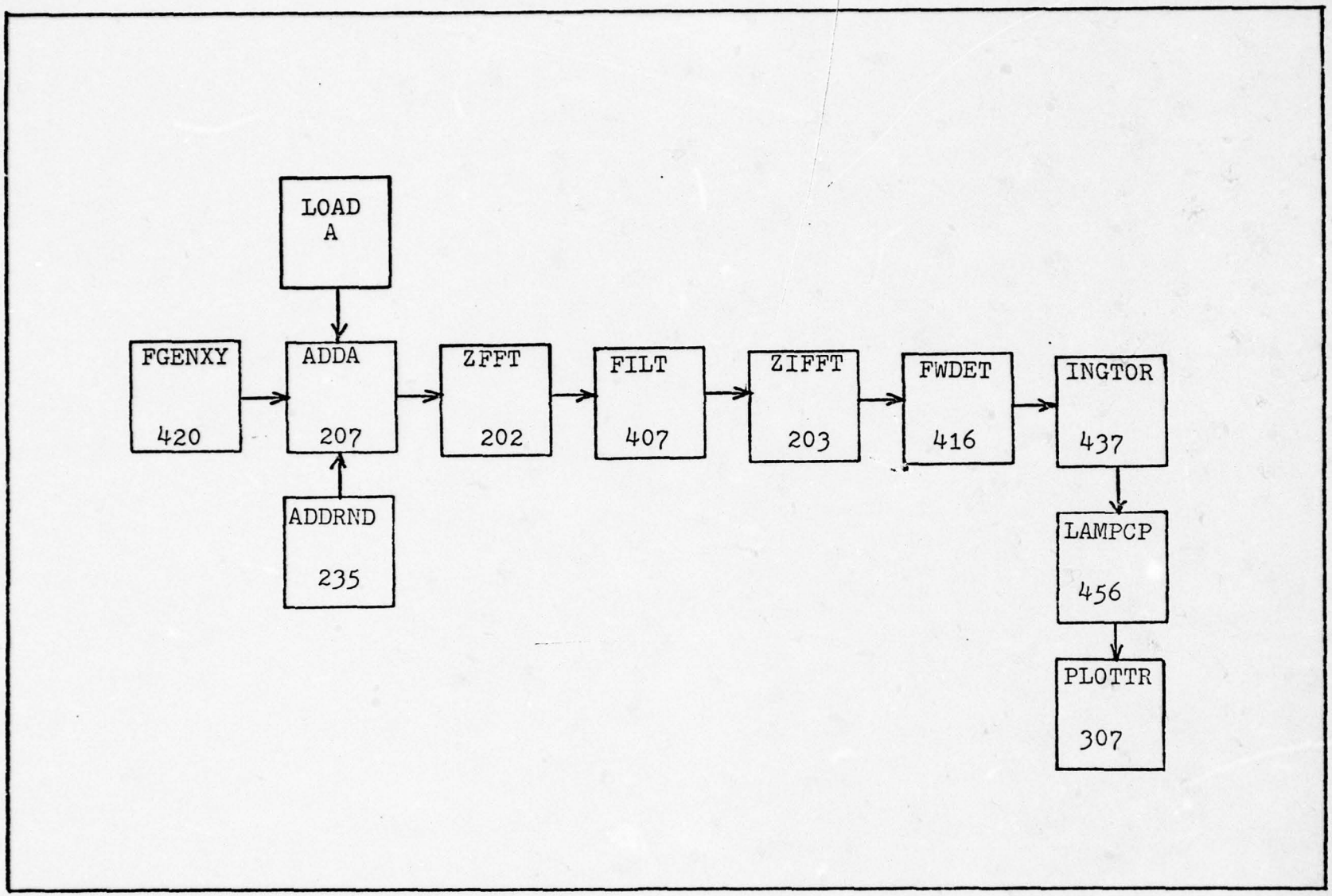

Figure 16. RADSIM Modules for Figure 12.

for these modules can be generated as parameter cards. ENDPAS, ENDCFG, ENDJOB cards are required at the end of the simulation control and parameter cards. If additional passes or configurations are run, ENDJOB is used only after the last pass or configuration. The only departure from the documented instructions for module parameter cards involves the graph labels for the plot subroutines Modules 307-310. Variables VIL, VDL and GLBL (independent variable label, dependent variable label, and graph label respectively) have been replaced with IVIL, IVDL, and IGLBL. The value of these variables should be set to the number of ten character words in the desired label (blanks included). The namelist must then be followed by a card containing a maximum of 80 characters for each label. IVIL, IVDL, and IGLBL and immediately reset to zero after reading the label card so that subsequent references to 307-310 need not contain labels. Figure 17 shows an example of this usage.

File Structure of RADSIM on the CDC 6600

The RADSIM Program is stored in the CDC 6600 computer (CSA) under an ASD/EN problem number. The source versions of the two main programs are cataloged as SLOADR and SSIMEX and the object versions of these programs as OLOADR and OSIMEX. Subroutines are stored in source form on a file named SPADLIB. The subroutines may be located for modification in the Page function of Editor. There are two

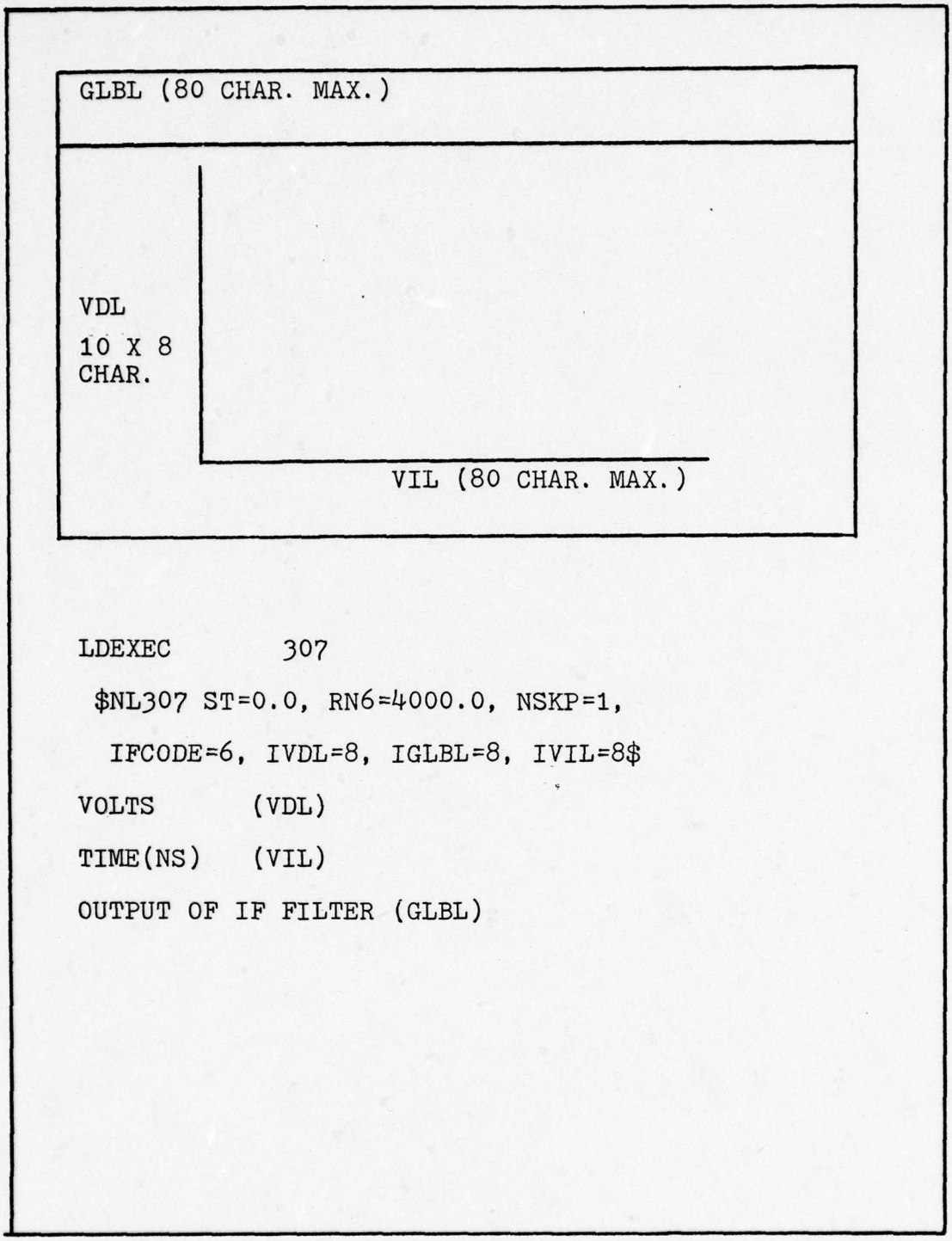


```
LDEXEC        307
 $NL307 ST=0.0, RN6=4000.0, NSKP=1,
  IFCODE=6, IVDL=8, IGLBL=8, IVIL=8$
VOLTS       (VDL)
TIME(NS)    (VIL)
OUTPUT OF IF FILTER (GLBL)
```

Figure 17. Graph Label Control Card Usage

Libraries of object subroutines. ORADLIB, contains those subroutines which must be executed with OLOADR to produce the data file for execution. ORALIB1 contains all the subroutines used with the simulation execution OSIMEX. Any job could run using ORALIB1/SSIMEX, but at least 275K of core would be required. A more efficient method is to create a new library containing only the necessary subroutines for the job. The RADSIM documentation suggests some alternate subroutine groupings which might offer advantages.

Core and Time Requirements

An average RADSIM job requires approximately 225000_8 words of central memory and 35-40 seconds per pass through the simulation. To permit more accurate estimates, calls to SECOND, and TIME are included in the SIMEX program. Use of a partial load map can also assist in estimating additional memory requirements for job extensions. System usage can be reduced by executing data decks with the loader (OLOADR and ORADLIB) only to verify their correctness. In this way errors in variable names in the namelists can be found and corrected prior to full scale execution. About 70K of core and less than ten seconds of CPU time should be sufficient for normal jobs of this nature. Experience with the ASD computer center operation indicates that normally a full RADSIM job will only execute overnight unless special priorities are obtained.

Suggested Changes to RADSIM

The following are changes which have not been performed but would inhance simulation integrity or operation.

a) Convert all in-MODULE code "ignore-type" code to calls to BOOL or IBOOL.

b) Check out all remaining FORMATS for incorrect word size in O or A FORMATS.

c) Consider some form of segmentation or overlaying to reduce core requirements. This may be complicated by large common area requirements.

d) Consider taking advantage of the increased precision of the 60 bit word over the 36 bit word.

Verification of Correct Performance

Since the purpose of this thesis included the simulation of synchronized pseudo-random noise against a DICKE-FIX radar receiver, the DICKE-FIX Sample Problem of Volume I Part 3 was used as verification of the simulations correct performance. Figures 18 and 19 show the comparative results on the Honeywell and CDC computers. The input values were the same, and the outputs were very close. The data from the CDC was hand plotted while the HIS data was plotted on an HP9820 calculator and x-y plotter. Since this is essentially what will be run for the experiment, the simulation was deemed correct for this case.

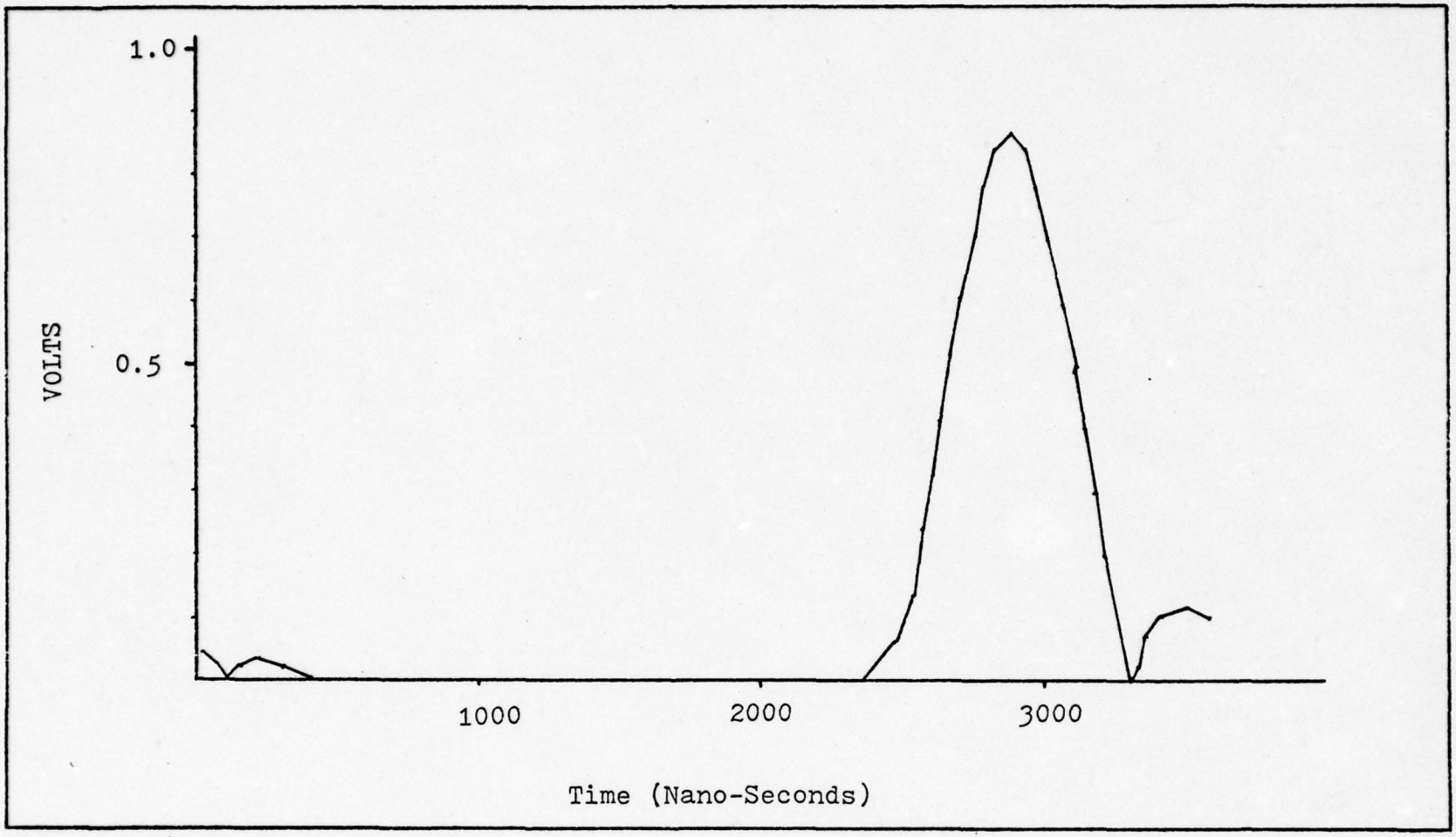

Figure 18. RADSIM Response

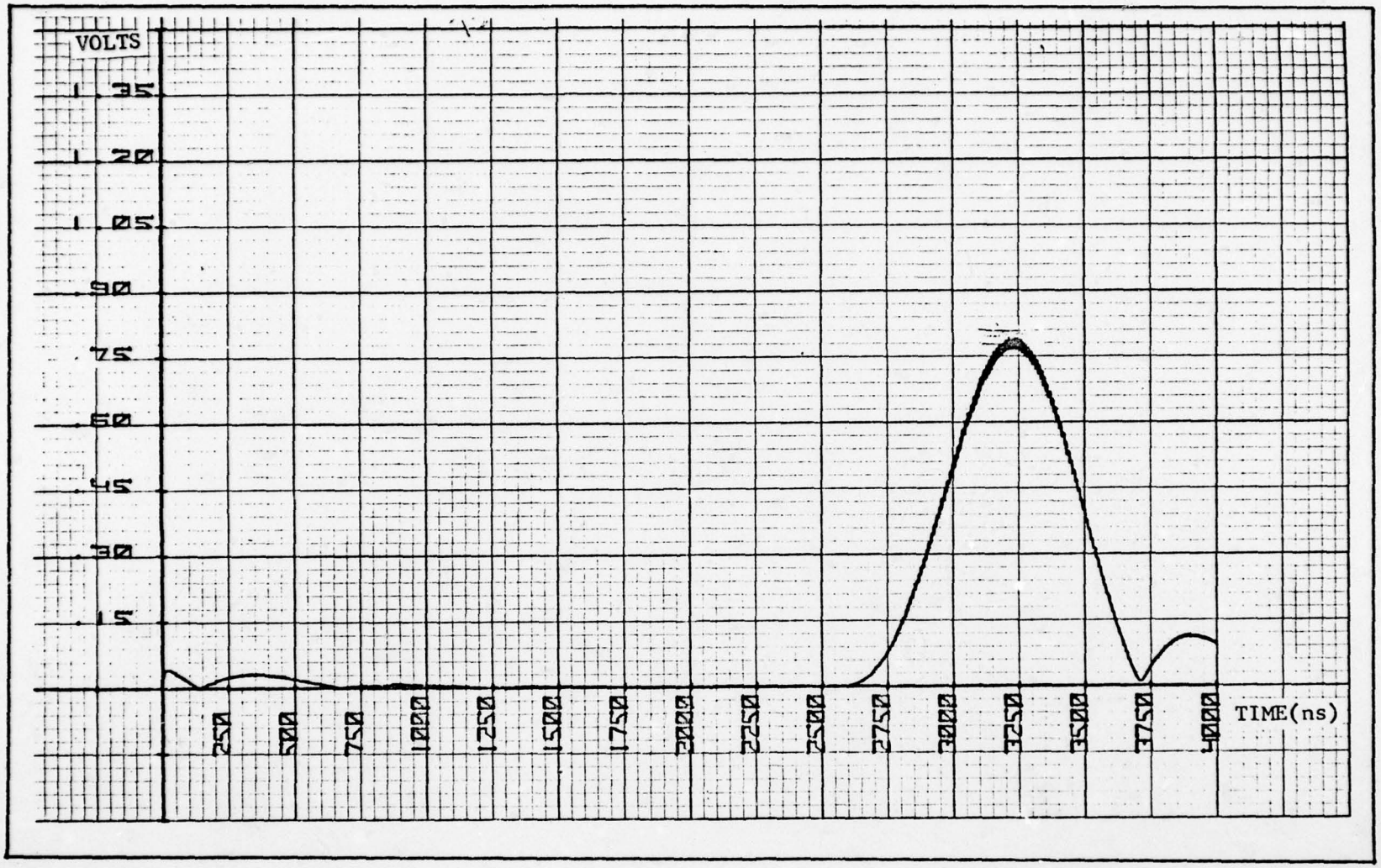

Figure 19. Response of RADSIM to TGT Pulse

IV. Experiment Design

The second major task of this study is to examine the effectiveness of synchronized pseudo-random noise jamming when employed against a radar equipped with a simple ECCM device, the DICKE-FIX. To do this an experiment will be performed using the RADSIM program. This section will describe the design of the experiment. The five phases to be covered are:

1) Selection of the radar paremeters.
2) Selection of radar model parameters.
3) Design of a synchronized pseudo-random noise jammer.
4) Set-up of the RADSIM model.
5) Specification of the experimental procedure.

Radar Parameters

The parameters of the victim radar for this experiment are shown in Table II. Only the receiver and display subsystems are to be modeled. Since the RF waveform carries no significant information it will be neglected (Ref 2:208).

Table II
Radar Parameters

Intermediate Frequency (IF)	20 MHZ
IF Bandwidth	1 MHZ
Pulse Repetition Frequency	300 PPS
Pulse Width	1200 Nano-seconds
Integration Efficiency	0.95

The intermediate frequency and bandwidth are chosen to be representative of search radars which might be encountered in USAF operations. They do not correspond to any specific system. The pulse width was set using the relationship (Ref 7:47):

$$\tau = 1.2/B = 1200 \text{ ns.} \qquad (4\text{-}1)$$

where: B = radar bandwidth

τ = radar pulse width

With the basic radar parameters of interest specified, the receiver system block diagram can be drawn. Using the model of Table II, the radar receiver subsystem is shown in Figure 20. The target return signal, thermal random noise and jamming are summed at the input of the receiver. The signal then passes through the wideband limiter (bandwidth > 10 MHZ), is filtered at the intermediate frequency to recover the target signal, and then is detected using a full wave detector. The energy in the signal is integrated to form a single pulse waveform and amplified by some arbitrary gain. This amplified signal is then applied to a post-detection video sweep integrator which integrates eight pulses for the display. Four cases will be considered in this experiment:

1) Thermal random noise only
2) Target plus thermal random noise
3) Thermal random noise plus synchronized pseudo-random noise jamming
4) Target plus thermal random noise plus synchronized

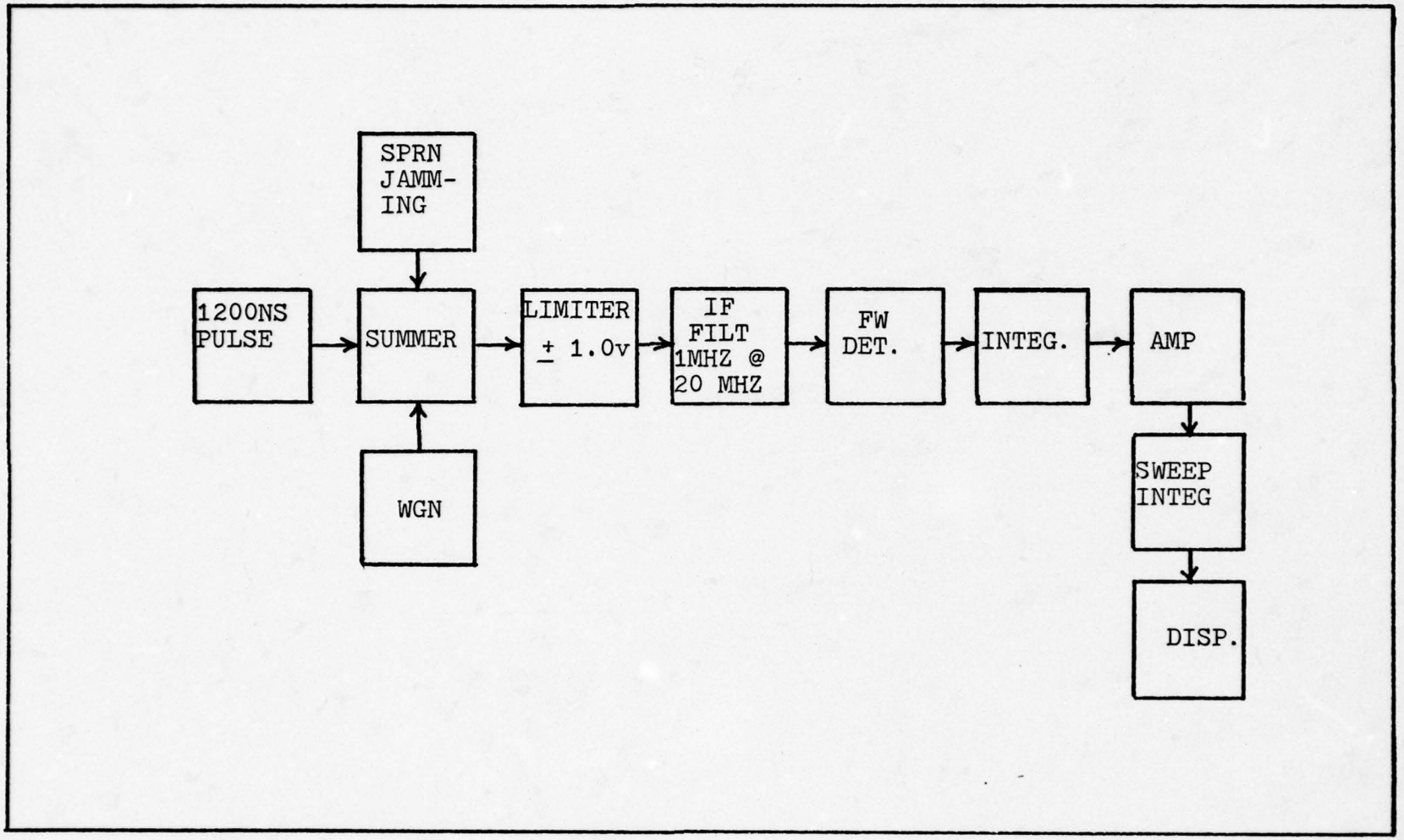

Figure 20. Radar Receiver Model

pseudo-random noise jamming

Radar Model Parameters

To implement the radar model, the parameters of each element must be specified. Some of the elements, the wideband limiter, the target signal shape, and the IF filter parameters are characteristic of the radar and will remain unchanged in any iteration of the experiment. Others such as the linear amplifier gain and the integration efficiencies of the two integrators may be varied but are not critical parameters for this investigation and will remain fixed throughout the experiment. The peak voltage of the target signal and the mean and variance of the noise, both thermal and SPRN are parameters which may be adjusted to provide the desired signal to noise ratios (SNR) for parametric analysis. Since the synchronized pseudo-random noise will be generated off-line to the simulation its characteristics will remain fixed.

The Wideband Limiter. The wideband limiter characteristic is that of a hard limiter. All positive input voltages become $+V_1$ and all negative voltages $-V_1$ (Ref 7:120). Figure 21 shows the voltage transfer function of the limiter. Its frequency characteristic is assumed linear over the bandwidth of the simulation.

The Intermediate Frequency (IF) Filter. The IF filter was selected to be a fourth-order Butterworth filter. This form is maximally flat in the passband and closely approximates the envelope of the power spectral density of the

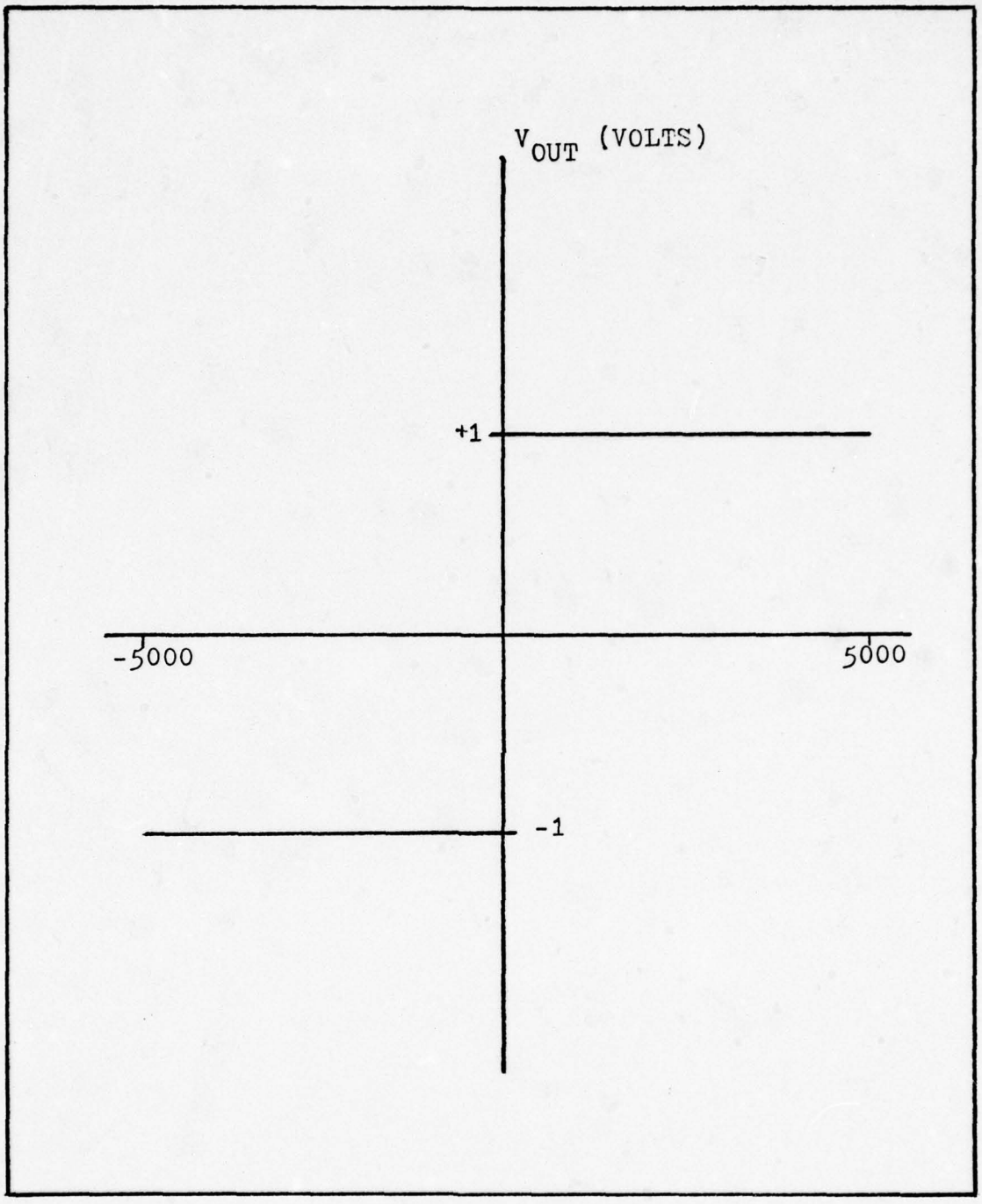

Figure 21. Voltage Transfer Function of Wideband Limiter. V_{OUT} is Undefined Beyond $\pm$ 5000 Volts V_{IN}.

rectangular pulse transmitted by the radar (Ref 11: 71). This can be shown by taking the Fourier Transform of the 1200 ns rectangular unit pulse.

$$S(t)=p[t,\ t-1200] \tag{4-2}$$

$$S(f)=1200\ \text{sinc}\ (1200f) \tag{4-3}$$

S(f), shown in Figure 22, closely approximates the form of the 4th order Butterworth filter shown in Figure 23. (Ref 11:71). The lowpass prototype of this filter is specified by a transfer function H(s).

$$H(S)=\frac{1}{S^4+aS^3+bS^2+cS+1}$$

where a, b, and c are coefficients which may be calculated or found in tables. In this case, the values from tables of Reference 11 were used. The prototype low pass filter is transformed to a bandpass filter by the frequency transformation:

$$S=\frac{s^2+\omega_o^2}{sB} \tag{4-5}$$

$s=j\omega$

ω_o=the center frequency of the bandpass filter

B=the bandwidth of the filter in radian frequency

The transformed filter response is then

$$H(s)=\frac{1}{\left(\frac{s^2+\omega_o^2}{sB}\right)^4+a\left(\frac{s^2+\omega_o^2}{sB}\right)^3+b\left(\frac{s^2+\omega_o^2}{sB}\right)^2+C\left(\frac{s^2+\omega_o^2}{sB}\right)+1} \tag{4-6a}$$

$$H(S)=\frac{s^4B^4}{s^8+As^7+Bs^6+Cs^5+Ds^4+Es^3+Fs^2+\omega_o^8} \tag{4-6b}$$

For simulation purposes these coefficients are calculated in terms of frequency rather than radian frequency

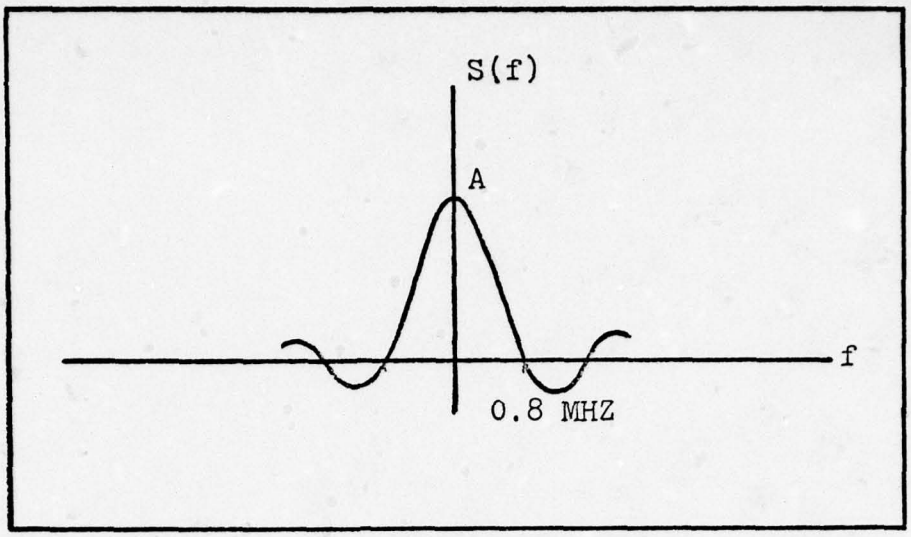

Figure 22. Fourier Transform of 1200 ns Pulse

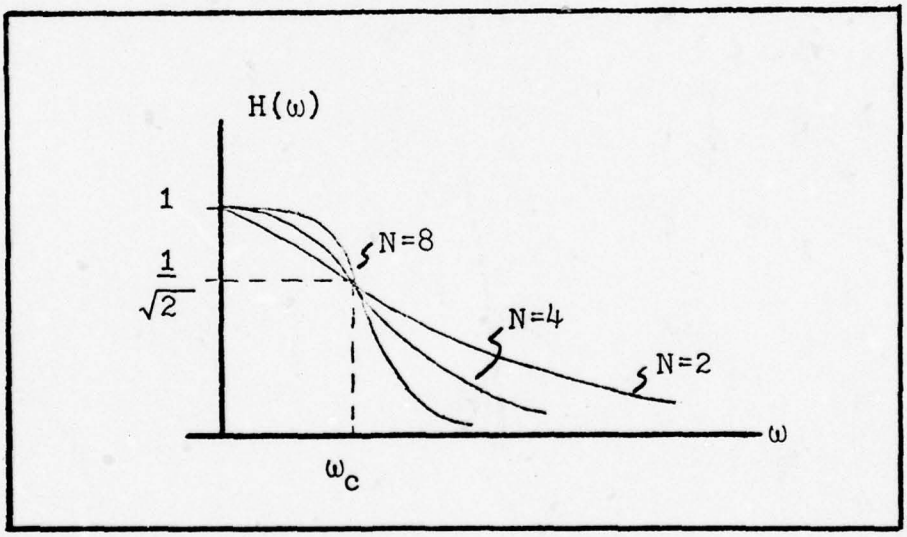

Figure 23. Butterworth Filter Magnitude Characteristics

and the units are in Gigahertz (10^9). Table III lists the coefficients.

Table III
IF Filter Transfer Function Coefficients

$A=ab=0.26131259X10^{-2}$

$B=bB^2+4f_o^2=0.16034142X10^{-2}$

$C=CB^3+3af_o^2B=0.31383642X10^{-5}$

$D=2B^2f_o^2+6f_o^4+B^4=0.96273237X10^{-6}$

$E=CB^3f_o^2+3aBf_o^4=0.12553457X10^{-8}$

$F=bB^2f_o^4+4f_o^6+0.25654627X10^{-9}$

$G=abf_o^6=0.16724006X10^{-12}$

$f_o^8=0.256000X10^{-13}$

$B^4=0.10000000X10^{-11}$

Factoring Equation (2-6b) with the AFIT PROGRAM POLY, provided the complex poles for the IF filter. Using another AFIT PROGRAM, FREQR, the filter was verified to have essentially unity gain at 20 MHZ with $\pm$3db points at 19.5MHZ and 20.5MHZ respectively. Figure 24 shows the filter transfer function plotted in the range 15-25MHZ.

Integration Efficiency. Integration efficiency will be set at 0.95.

Target and Noise Signal. The target signal is specified to be a rectangular pulse at the 20 MHZ center frequency of 1200 Nanoseconds duration. The rise time is specified as 10 Nanoseconds, and the peak value will be set so that its value relative to the measured noise output from

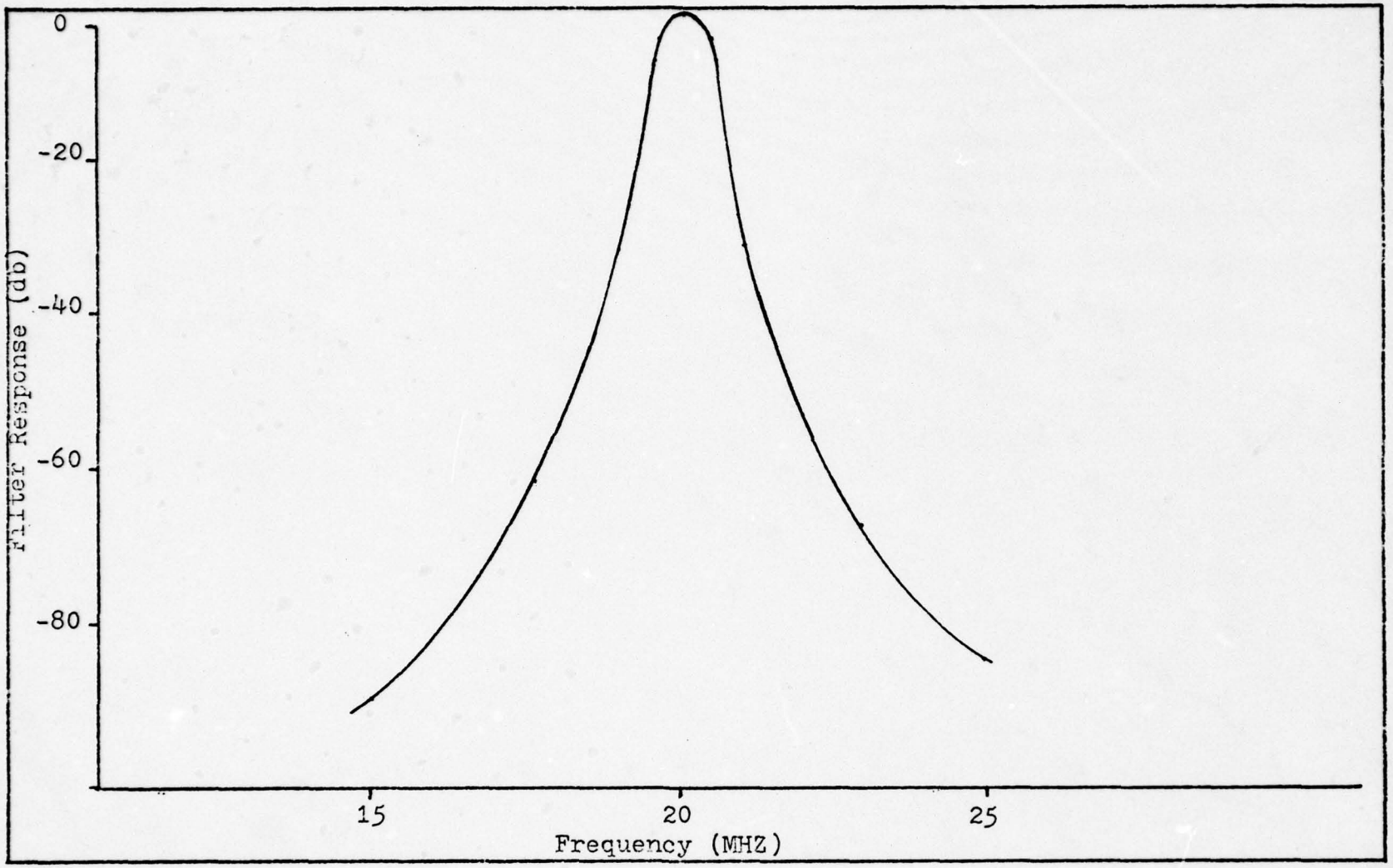

Figure 24. Response of IF Filter

the IF filter will provide the desired signal to noise ratio.

The Synchronized Pseudo-Random Noise Jammer

By the theory developed in Section II, there are two major constraints which must be met effective pseudo-random noise jamming. A bandwidth constraint which defines the point of the first null of the jamming noise-power spectral density function and a synchronization constraint that is imposed by the requirement that the period of the sequence equal the pulse repitition interval of the radar. These can be expressed as a pair of simultaneous equations in terms of the clock frequency of the shift register (Ref 2:138).

$$f_c=\frac{kBr}{2} \qquad (4-7)$$

$$f_c=2^r f_R$$

f_c=clock frequency

B=radar bandwidth

r=number of stages in the shift register

f_r=pulse repitition frequency of the radar

k=a constant to increase the bandwidth of the jammer by some factor to allow for inaccuracies in determining the radar parameters (set-on constant)

Figure 25 shows the results of plotting the values of these two equations for the radar parameters of Table II. Assuming that k=10 is a reasonable value for the set-on constant, the clock frequency and shift register length are 92MHZ and 18 respectively. By choosing the primitive irreducible

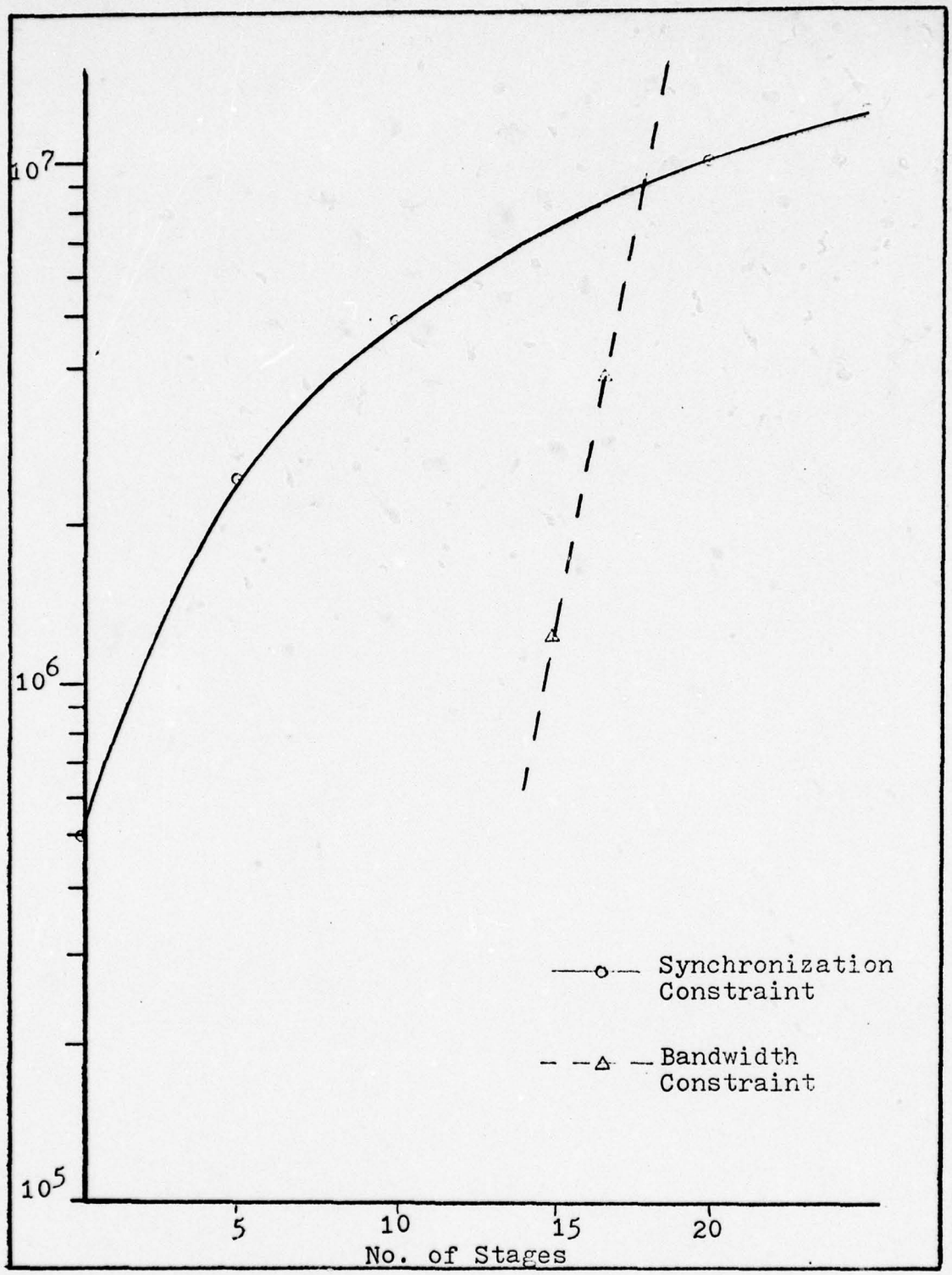

Figure 25. Plot of Synchronization And Bandwidth Constraint Equation Solutions

polynomial of degree 18 with the smallest number of non-zero terms from the Tables of ENAD TR-74-01 (Ref 5:97) the characteristic function is found to be:

$$f(x)=X^{18}+X^{11}+1 \qquad (4\text{-}9)$$

This leads to a shift register jammer of the form shown in Figure 6. This jammer was implemented in a computer program to provide 8192 samples values of the jamming signal in a 4000 observation interval around the received pulse. Appendix A describes to computer program PRN which calculates the sample values and stores them in a form suitable for RADSIM.

The RADSIM Model

Figure 26 shows the radar model of Table II specified in terms of RADSIM Module Reference Numbers. Table IV describes the modules and their specific functions. It also specifies the sequence in which the modules are to be executed. Appropriate output modules have been added to allow examination of the wave forms at two points in the simulation. Table V lists the control cards and simulation cards necessary to perform the simulation. Figure 27 shows the data flow for simulation execution. Note that the sampled data for the jamming wave form has been stored on a temporary file (TAPE 3), and is rewound and repeated every pulse repetition interval.

Experimental Procedure

The experiment will consist of two phases. The

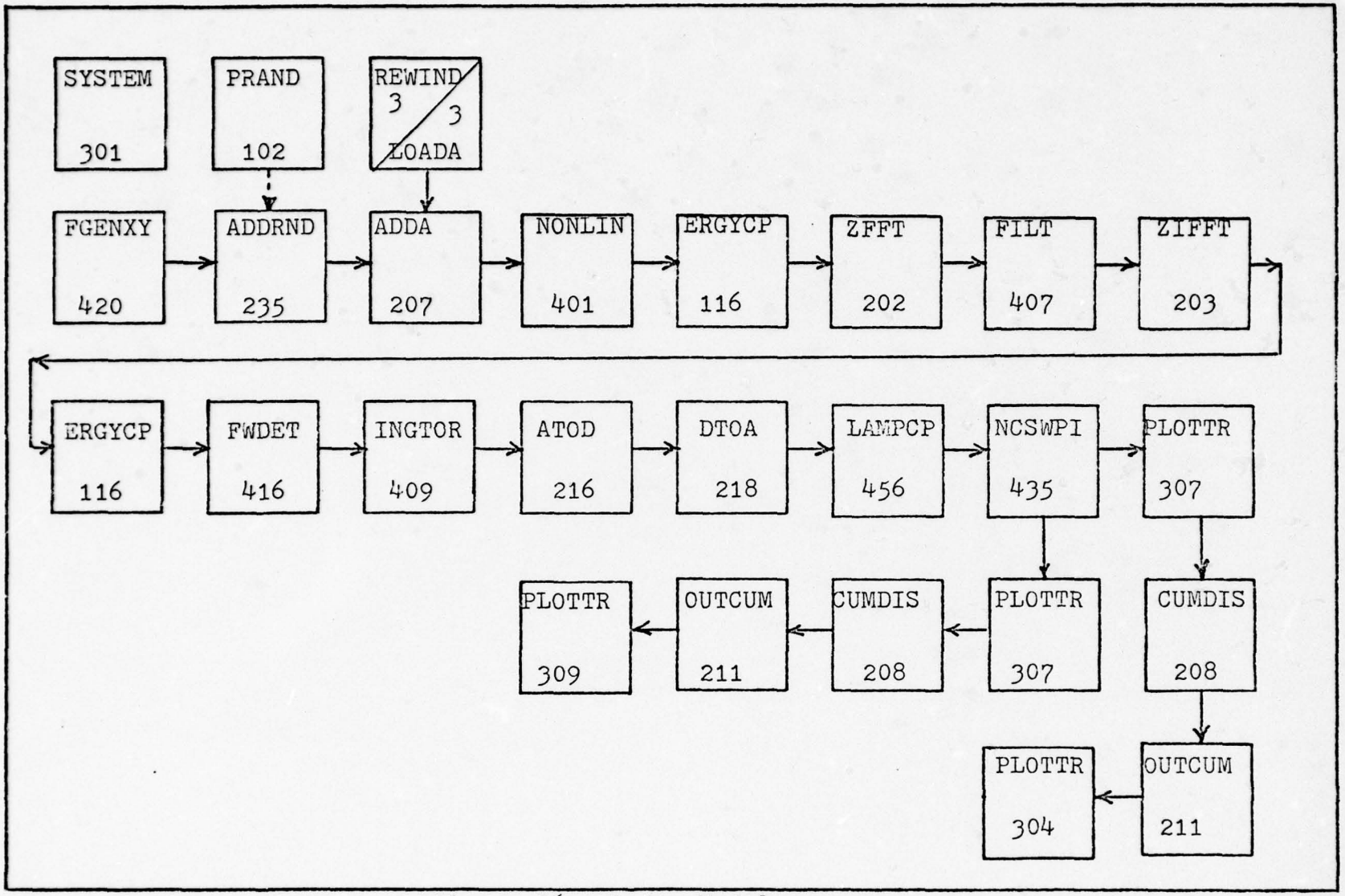

Figure 26. Radar Model as run

Table IV
Module Specifications and Sequence

Seq. No.	Module Name/MRN	Purpose/Specification
1.	SYSTEM/301	Initialize System Parameters
2.	RRAND/102	Initialize Random Number Generator
3.	FGENXY/402	Target Signal Generator
4.	ADDRND/235	Add Random Noise to Target Signal
5.	REWIND 3	Rewind PRN Jammer Sample File
6.	STOREA 3	Store Jammer Samples in Array XA
7.	ADDA/207	Add TGT + Noise + Jammer
8.	NONLIN/401	Wideband Limiter
9.	ERGYCP/116	Measure Input Energy
10.	ZFFT/202	Transform to Frequency Domain
11.	FILT/407	4th Order Butterworth Filter IMHZ BW @ ZOMHZ
12.	ZIFFT/203	Transform to Time Domain
13.	ERGYCP/116	Measure Output Energy
14.	FWDET/416	Full Wave Envelope Detector
15.	INGTOR/409	Integrator (.95 Efficiency)
16.	LAMPCD/456	Linear Amplifier
17.	* PLOTTR/307	Plot Presweep Integration Signal
18.	* CUMDIS/208	Generate Histogram of Signal Voltages

Seq. No.	Module Name/MRN	Purpose/Specification
19.	* OUTCUM/211	Generate Cumulative Distribution of Signal
20.	* PLOTTR/309	Plot CDF
21.	ATOD/216	Analog To Digital Conversion
22.	DTOA/218	D to A (Set Saturation Level, Reduce Number of Points)
23.	NCSWPI/436	Post Detection Video Sweep Integrator
24.	* PLOTTR/309	Plot Integrated Signal
25.	* CUMDIS/208	Generate Histogram of Integrated Signal
26.	* OUTCUM/211	Generate CDF of Integrated Signal
27.	* PLOTTR/309	Plot CDF

* Omitted on Passes 1-7 to reduce output requirements.

Table V
Control Cards for RADSIM Execution

JOB CARD

FTN. Used to Execute SPRN Generator

LGO. Not used W/WGN Cases

ATTACH OLOADR

ATTACH ORADLIB

ATTACH CC6600, ID=X654321, SN=ASD

LIBRARY ORADLIB, CC6600

OSIMEX

7/8/9/

SPRN Generator Source And Assembly Language Deck

7/8/9

DATA Card for SPRN Generator

7/8/9

Simulation Control Card Deck

6/7/8/9

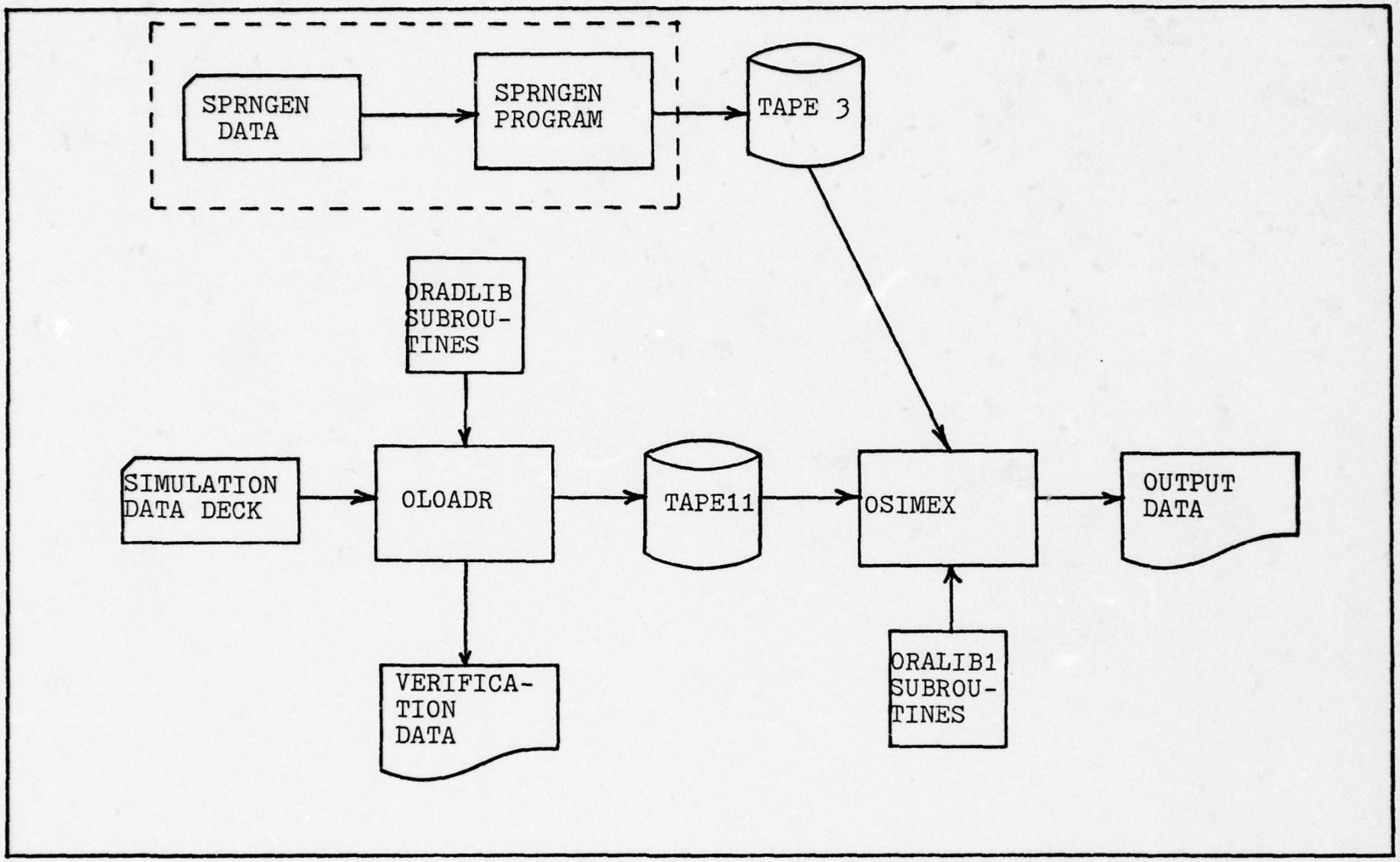

Figure 27. Data Flow as run

first phase will be calibration. The output of the IF filter (MRN203) will be measured for two cases, White Gaussian Noise (WGN) and WGN + Synchronized Pseudo-Random Noise. By calculating the energy density for each of these cases, the desired signal to noise ratio may be obtained by adjusting the target return signal voltage. A signal to noise ratio of 2 will be studied since it should show the largest change in performance (Ref 2:273). The final phase will be experimentation in which the simulation will be exercised for the cases shown on Table VI.

Table VI
Simulation Cases

1.	WGN (No DICKE-FIX)
2.	WGN (With DICKE-FIX)
3.	WGN + SPRN (No DICKE-FIX)
4.	WGN + SPRN (With DICKE-FIX)
5.	WGN + TGT (No DICKE-FIX) (SNR=2)
6.	WGN + TGT (With DICKE-FIX) (SNR=2)
7.	WGN + TGT + SPRN (No DICKE-FIX) (SNR=2)
8.	WGN + TGT + SPRN (With DICKE-FIX) (SNR=2)

Using the data gathered from this sequence of simulations, a set of receiver operating characteristic (ROC) curves will be constructed for cases five through eight. These ROC's will be used to verify the theory and demonstrate the effectiveness of synchronized pseudo-random noise jamming against the DICKE-FIX receiver.

V. The Experiment, Data Analysis, and Results

In this section the conduct of the experiment will be explained and the data obtained analyzed. There were two major phases to the experiment, as described in Section IV. The first consisted of a series of measurements to determine the amount of energy present in the White Gaussian Noise (WGN) and Synchronized Pseudo-Random Noise (SPRN) signals so that an appropriate target signal amplitude could be established, and related to the signal to noise (SNR) ratio of Dr. Berrie's experiments. The second phase consisted of running each of the cases described on Table VI of Section IV with the appropriate target signal amplitude. Simulation output data consisted of the cumulative probability distribution of the pre and post-integration signal voltages for the eighth pulse. The data was recorded in both graphical and point list form. This data was converted to P_{fa} and P_d curves similar to Figure 11, and an ROC was drawn for each case. These ROC's were then compared to the data obtained in Berrie's experiments and related to the analytical values he established.

Determination of WGN Energy Levels

Reference 3 provides a formula for establishing the energy of WGN noise generated by the simulation.

$$E = (2^{N^2})(\sigma^2)(1/FS)(\text{Watt-Nanoseconds}) \qquad (5\text{-}1)$$

where: E = total energy

2^{N^2} = no. of samples as determined by input parameters ($2^{N^2}=2^{13}=8192$

σ^2 = noise variance

FS = sample rate

Energy density can then be determined using the energy obtained from Equation (5-1).

$$N = E/FS \ (\text{Watt-Nanoseconds/GHZ}) \qquad (5\text{-}2)$$

N = energy density

The value selected for the noise variance was 0.5, the sample rate was 2.0 GHZ, and N^2 was 13. Thus by (5-1) and (5-2), including the factor (2400/4096) to account for the sampling of energy during the target pulse only:

$$E = (2^{13})(0.5^2)(1/2)(2400/4096) = 600 \text{ W-NS} \qquad (5\text{-}3a)$$

$$N = 600/2 = 300 \text{ W-NS/GHZ} = 0.3\frac{\text{W-NS}}{\text{MHZ}} \qquad (5\text{-}3b)$$

Measurement of ten independent runs of WGN, taking the energy of the signal at the input and output of the IF filter, provided the data of Table VII. Each run consisted of eight passes through the simulation with only the mean and standard deviation of the energy's obtained shown.

Table VII
Statistics of Ten Independent White Gaussian Noise Sample Sets Into and Out of the IF Filter

IDENT	E_{IN}(Ei)W-NS		E_{OUT}(E_o)W-NS	
	MEAN	STD DEV	MEAN	STD DEV
FMA	593.40	25.17	0.41	0.24
FMB	602.87	15.22	0.70	0.34
FMC	599.03	9.92	0.65	0.51
FMD	588.08	13.79	0.67	0.31
FME	595.54	8.95	0.37	0.28
FMF	602.73	16.94	0.62	0.23
FMG	600.57	11.35	0.71	0.27
FMH	602.91	12.53	0.69	0.44
FMI	601.85	12.73	0.49	0.20
FMJ	594.46	13.47	0.25	0.52

Calculating the mean and standard deviation of these samples gave:

$$\bar{E}_i = 598.14 \qquad S = 5.06 \tag{5-4a}$$

$$\bar{E}_o = 0.56 \qquad S = 0.16 \tag{5-4b}$$

$$\bar{n} = 0.29907 \text{ Watt-Nanoseconds/MHZ} \tag{5-4c}$$

These values of $\bar{E}_i$ and $\bar{n}$ compared favorably with the theoretical value of Equations (5-3a, 5-3b). The noise bandwidth (B_N) of the receiver model was then computed using Equation (5-5).

$$B_N = \bar{E}_o/n \qquad (5\text{-}5)$$

$$= 0.56/0.30$$

$$= 1.87\text{MHZ}$$

Since the signal energy and noise energy are measured over the same period, the ratio of signal power to noise power (SNR) is equivalent to the ratio of signal energy to noise energy. For a noise bandwidth of 1.87 MHZ, the energy ratio at the input to the IF filter, equivalent to a post IF filter SNR of 2, is

$$\frac{E_s}{\bar{E}_o} = \frac{E_s}{nB_N} = Z \qquad (5\text{-}6a)$$

$$E_s = (2)(1.87)(0.3) = (2)(1.87)(0.3) \qquad (5\text{-}6b)$$

$$= 1.122 \text{ Watt -Nanoseconds}$$

Signal amplitude was then calculated using Equation (5-7)(Ref 14:321).

$$E_s = 1/2\ A^2T \qquad (5\text{-}7)$$

A = signal amplitude

T = signal deviation

For E_s = 1.122 Watt -Nanoseconds and T = 1200 Nanoseconds (from Table II):

$$A = \sqrt{\frac{2}{T}\ (E_s)} \qquad (5\text{-}8)$$

$$= \sqrt{\frac{2}{1200}\ (1.122)} = 0.043 \text{ volts}$$

The value of A from Equation (5-8) was then used as VPEAK for a SNR = 2 in White Gaussian Noise.

Since the amount of energy within the IF filter band-

width varied from run to run, a high value, low value and near mean value were chosen to be run for the experiment. The high was obtained from run FMG, the low from FMJ and the closest to the mean from FMF.

Determination of Synchronized Pseudo-Random Noise Energy Levels

To determine the energy present in the SPRN jamming signal a calculation was performed using a formula from the users manual for the Hewlett Packard 3722A Noise Generator (Ref 13:3-7). Its characteristics are very similar to the noise generator used in this experiment. The Noise Power Density of the Pseudo-Random Noise generator is given by Equation (5-9).

$$NPD = 2a^2 T \qquad (5\text{-}9a)$$

NPD = noise power density in V^2/HZ

a = the shift register amplitude

T = the clocking rate of the shift register

Thus:

$$NPD = (2)(1)(^1/92X10^2) = 2.174 \text{ X } 10^{-2} \text{ } V^2/HZ \qquad (5\text{-}9b)$$

Energy density is the product of the noise power density times the interval over which the measurement is taken, so by Equation (5-10)

$$E = (NPD)(Time) \qquad (5\text{-}10)$$

$$= (2.174 \text{ X } 10^{-2} \text{ Watts})(2400 \text{ N.S.})$$

$$= 521.8 \text{ Watt - Nanoseconds}$$

To measure the actual output, the noise generator was cycled through a full period and the register state sampled

every 377 shifts. Ten of these states were selected at random and used as the starting point for a simulation. The average energy for each of these runs and the standard deviation is shown in Table VIII.

Table VIII
Statistics of Ten Independent
Pseudo-Random Noise Jamming Signals

IDENT	E_{IN}(Ei)W-NS		E_{OUT}(E_o)W-NS	
	MEAN	STD DEV	MEAN	STD DEV
FMK	771.64	18.34	25.74	2.45
FML	707.54	14.30	8.36	2.10
FMM	689.50	9.64	7.95	1.07
FMN	679.90	12.70	7.66	1.78
FMO	691.01	14.63	7.03	1.40
FMP	692.76	11.13	10.79	1.90
FMQ	731.72	13.28	10.51	1.52
FMR	669.68	10.45	5.28	0.94
FMS	690.29	12.86	55.08	4.28
FMT	691.98	14.84	11.21	2.30

Averaging these samples provided a mean energy into the IF filter of 701.59 Watt- Nanoseconds and a mean energy out of 14.96 Watt- Nanoseconds. Standard deviations were 29.62 Watts- Nanoseconds and 15.20 Watt - Nanoseconds respectively. These values of means did not compare closely to the calculated value of energy in the SPRN signal from Equation (5-9). Equation (5-9) however assumed that the entire sequence was generated. Berrie showed that for short

subsequences of maximal length sequences, the Chi-square value can be very high (Ref 2:109). One would therefore, not expect any individual sequence to demonstrate an exact correspondence to the full sequence. Further verification of this property was shown by taking the average value of the modulating signal for one of the runs. For a true maximal length sequence the average value should be very close to zero. Examination of the average values of the subsequences showed a distinct bias which would add some energy to the waveform that would not exist for a true maximal length sequence. There were 695 possible independent subsequences of which only ten were chosen. It is quite possible that examination of more subsequences would produce an average value closer to the computed value.

The target signal amplitude was set in the same manner as for White Gaussian Noise, using the calculated values for energy and energy density. The bandwidth (B_j) of the jammer was 10.22 MHZ. Thus:

$$n_{SPN} = E/B_j \tag{5-11}$$

$$= 521.8/10.22$$

$$= 51.1 \ \frac{\text{Watt}}{\text{MHZ}} - \text{NS}$$

Substituting into Equation (5-6a)

$$E_s = n_{SPN} B_N 2 \tag{5-12}$$

$$= (2)(1.87)(51.1)$$

$$= 191.15 \text{ Watt} - \text{NS}$$

And computing the amplitude A as in Equation (5-8)

$$A = \sqrt{\frac{2}{1200}(191.15} = 0.56 \text{ volts} \qquad (5\text{-}13)$$

VPEAK for the Synchronized Pseudo-Random Noise cases was set at 0.56 volts.

Table VIII showed that the amount of energy in the IF filter bandwidth varied greatly and no mean value was ever generated. Two samples were used. FMK and FMT bracketed the calculated mean value.

Conduct of the Experiment

Each case was run using the parameters which defined the energy levels and the appropriate target signal voltage. Limits on the output data histogram elements were changed as necessary. Each case from Table VI was generated.

Results and Analysis of the Data

The data from the simulation consisted of a point list and graph describing the cumulative probability distribution (c.p.d.) of the voltage levels both into and out of the pulse integrator for the eighth pulse integration. The c.p.d. indicated the probability that any voltage would be less than a specified voltage, as shown in Equation (5-14) and Figure 9.

$$P(v<V) = \int_0^V f(v)\, dv \qquad (5\text{-}14)$$

Probability of detection or false alarm as defined in Equations (2-23) and (2-24) may be calculated from the simula-

tion c.p.d. by simply subtracting any value on the c.p.d. from 1. A pair of curves representing P_{fa} and P_d were developed for each sample case as shown in Figure 11. These curves were then used to generate a Receiver Operating Characteristic Curve that combined the pre and post-integration performance of the individual sample case. For WGN there was a high, low, and near mean sample for each case. In the SPRN cases there was a high mean and a low mean sample. These samples were averaged to produce an average Receiver Operating Characteristic curve for each of the cases five through nine of Table VI. These ROC's are shown in Figures 28 through 31. Each performance curve was also compared to Berrie's data to evaluate the correspondence between the RADSIM simulation and the values obtained from theory and analog experiments. Figures 32 through 35 show these comparisons. Performance comparisons for the cases with and without the wideband limiter are made in Figures 36 through 37.

Discussion of Results

A true ROC should go to zero in its lower left hand corner indicating $P_{fa} = P_d = 0$. The non-zero value of the observed ROC's is due to truncation of simulation values to fit into discrete histogram elements, of which there are only a finite number. Better data could be obtained in these ranges by selecting different histogram parameters. All of RADSIM ROC's exhibited this characteristic.

Figures 32 through 35 show that the RADSIM results

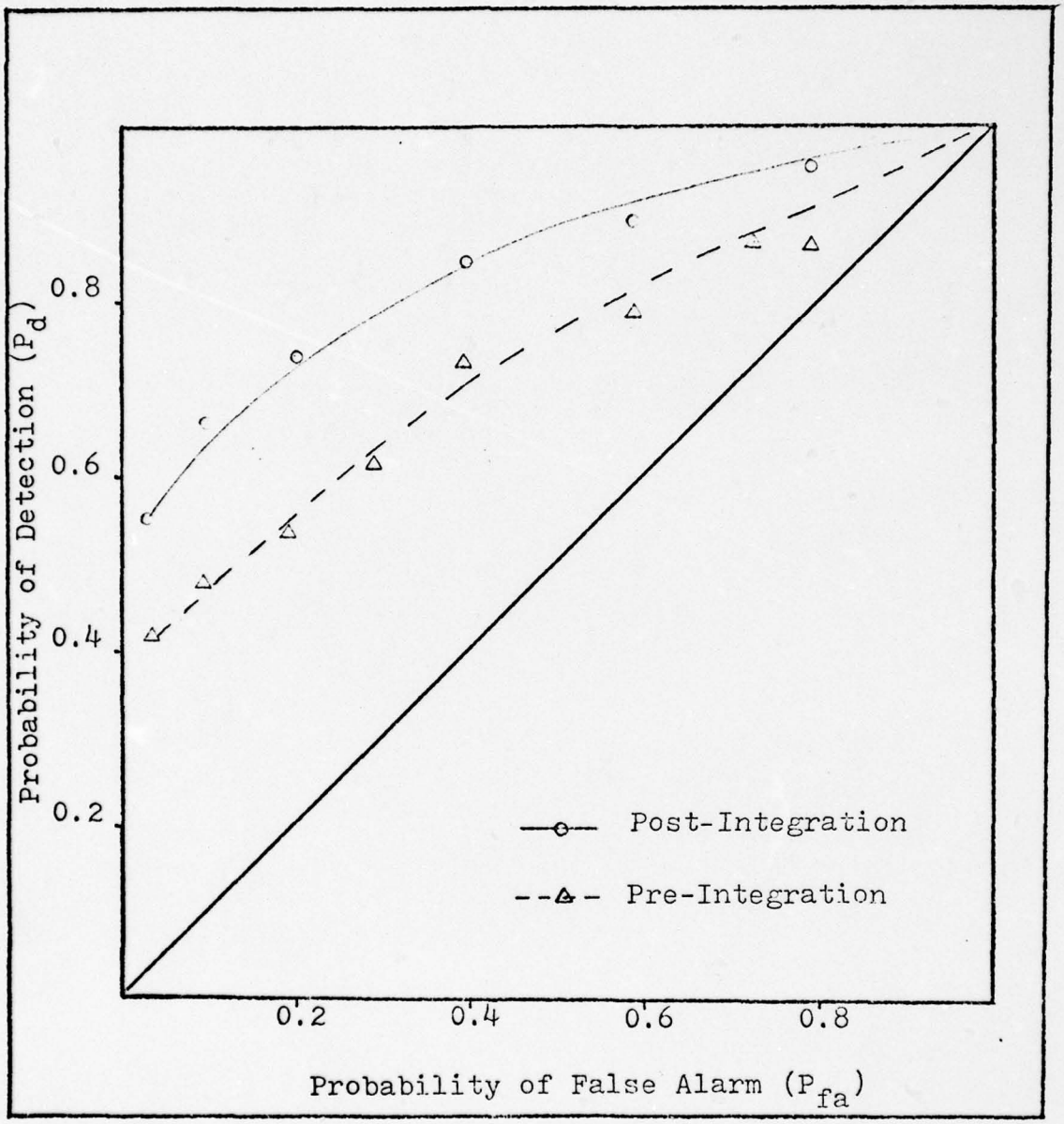

Figure 28. Average Performance in WGN

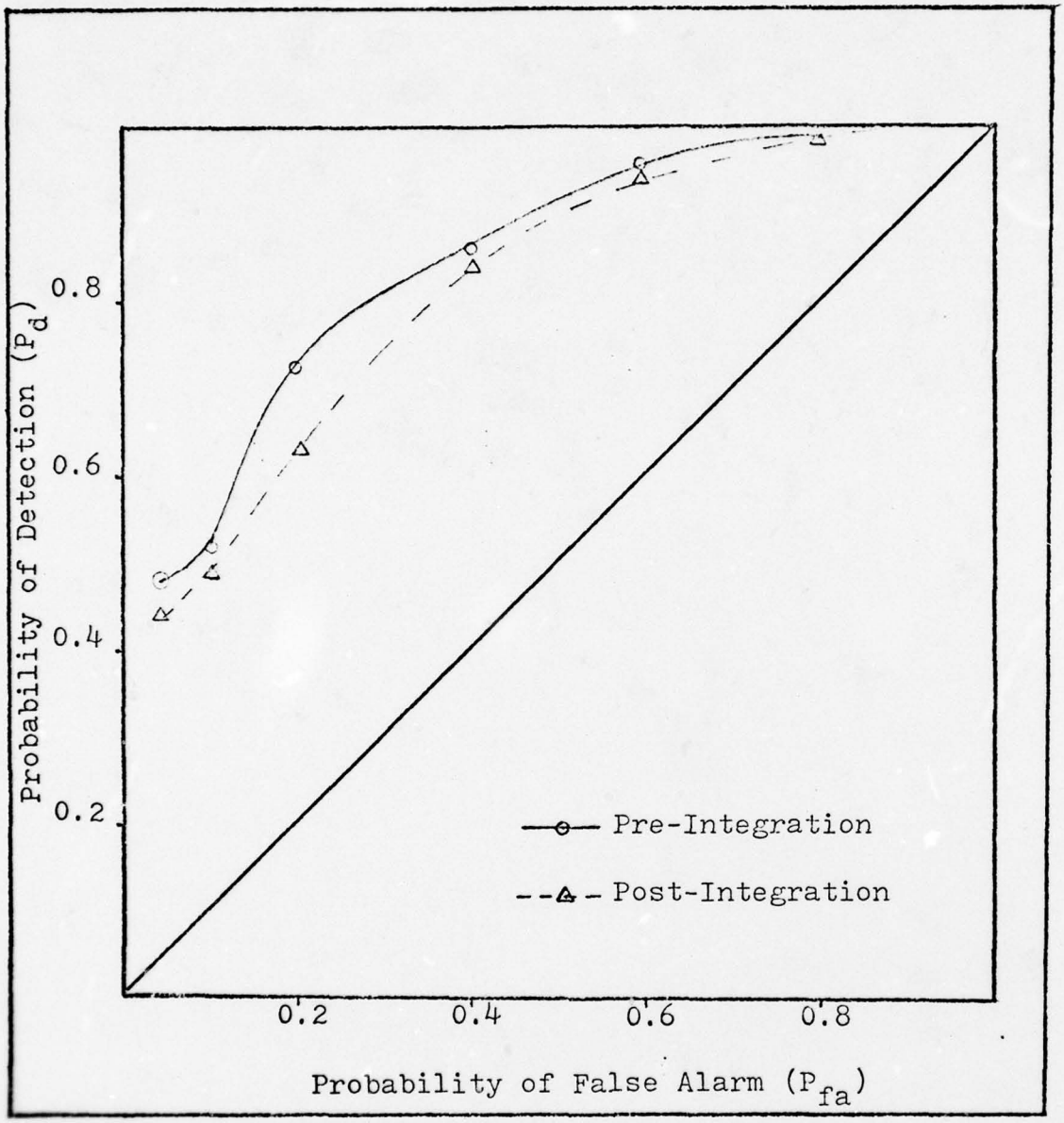

Figure 29. Average Performance in Synchronized Pseudo-Random Noise

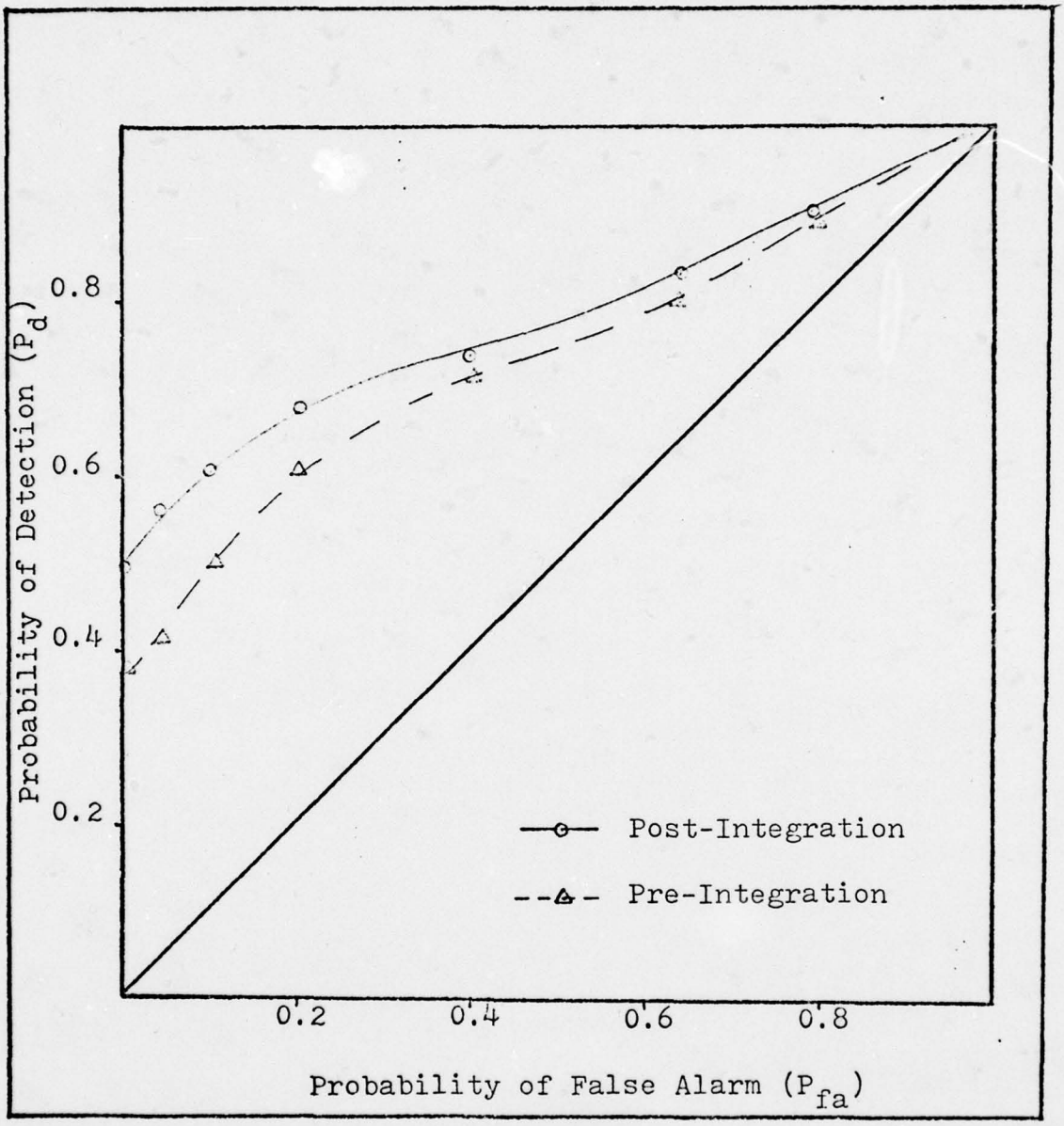

Figure 30. Average Performance in WGN With Limiting

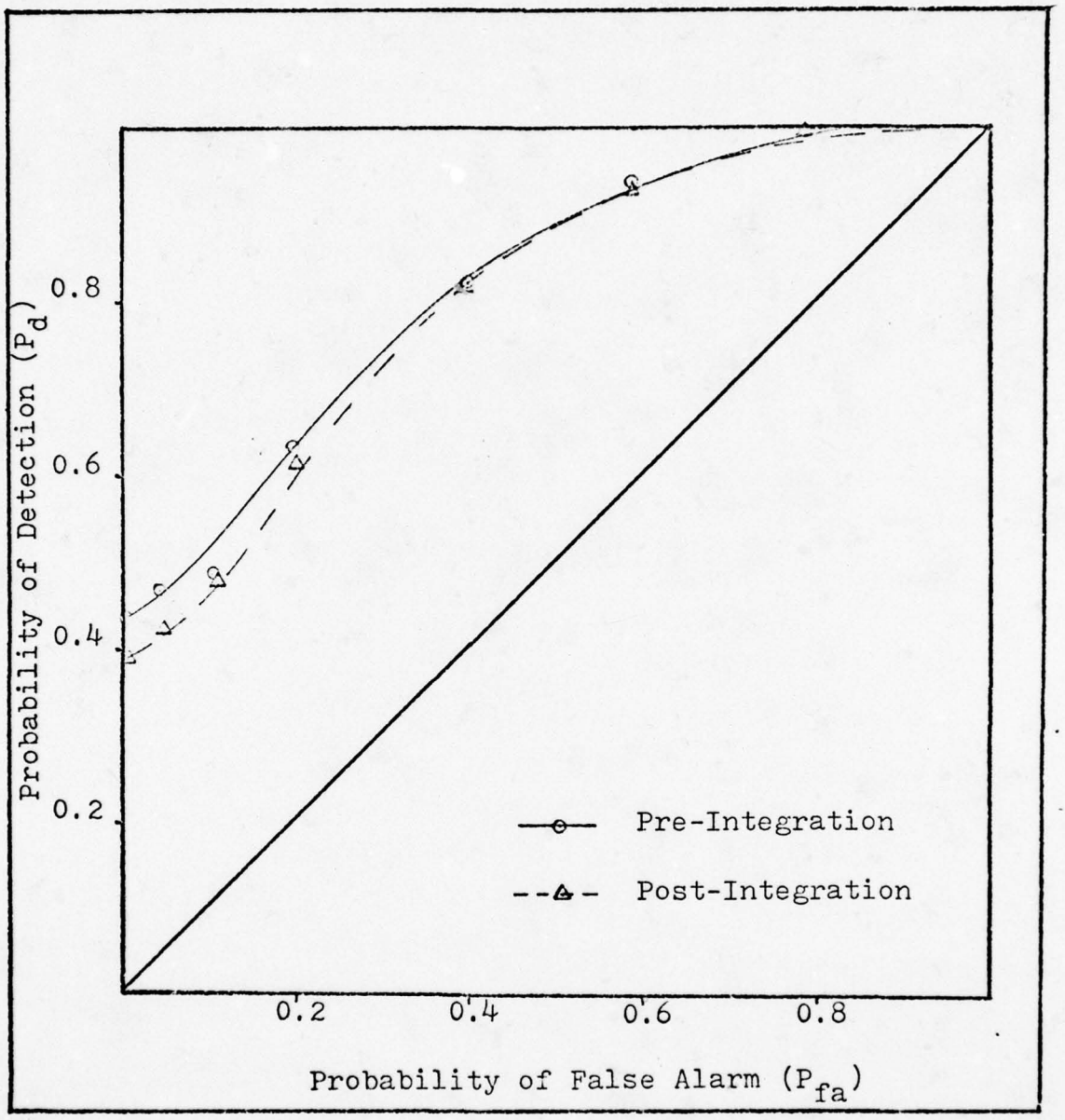

Figure 31. Average Performance in SPRN With Limiter

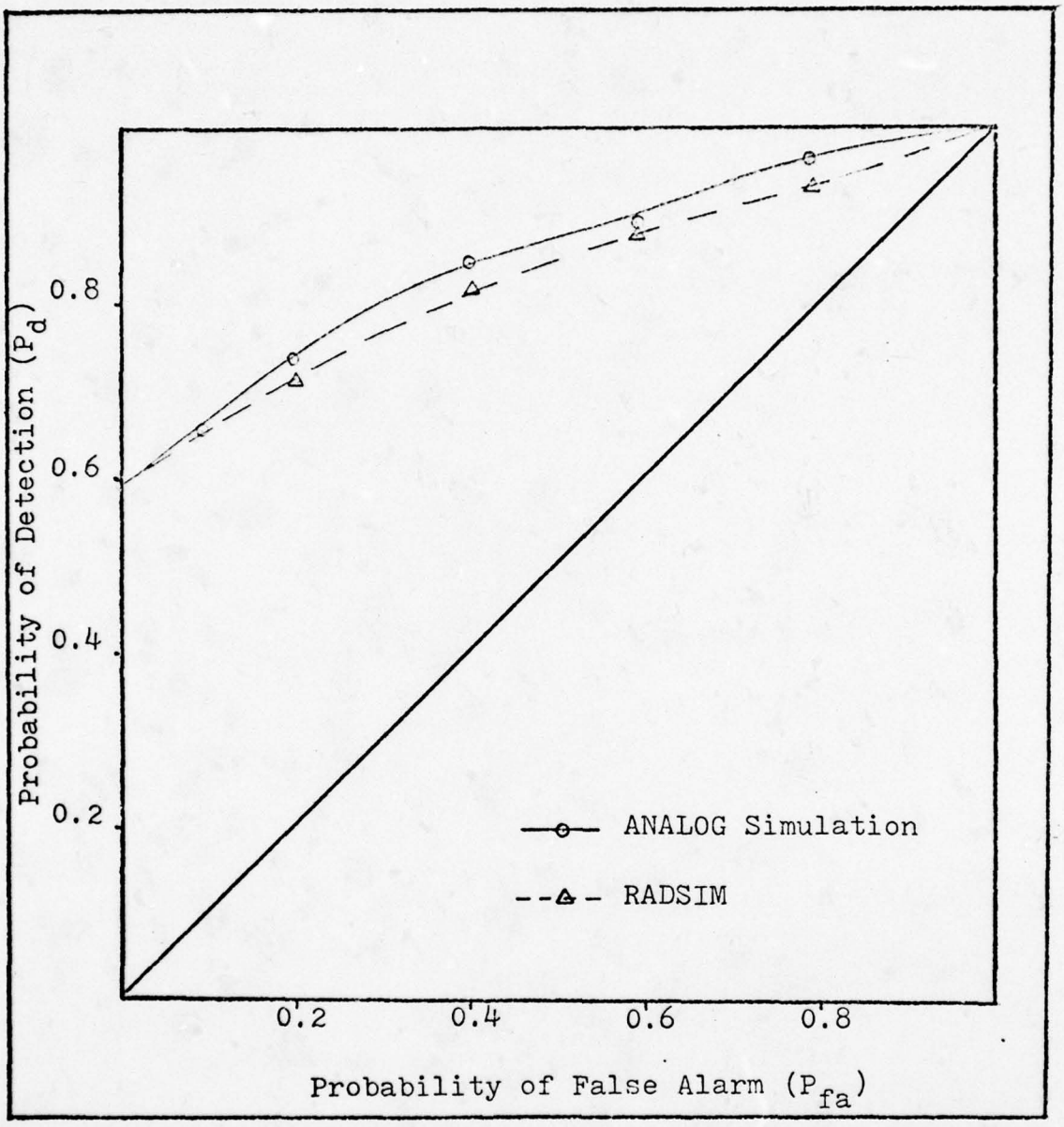

Figure 32. Comparison of Average Post-Integration Performance, in WGN. RADSIM vs. ANALOG Simulation.

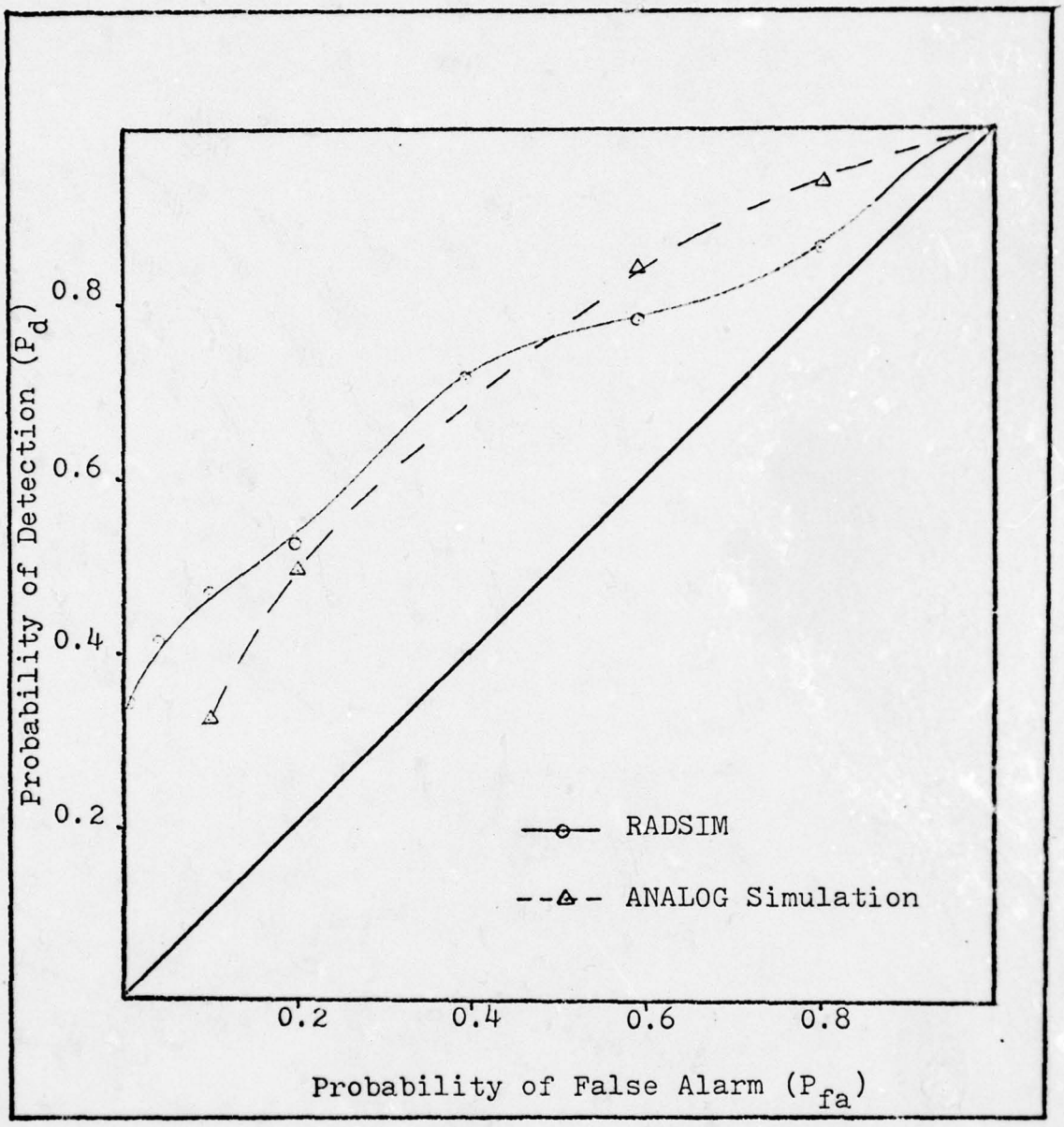

Figure 33. Comparison of Average Pre-Integration Performance, in WGN. RADSIM vs. ANALOG Simulation.

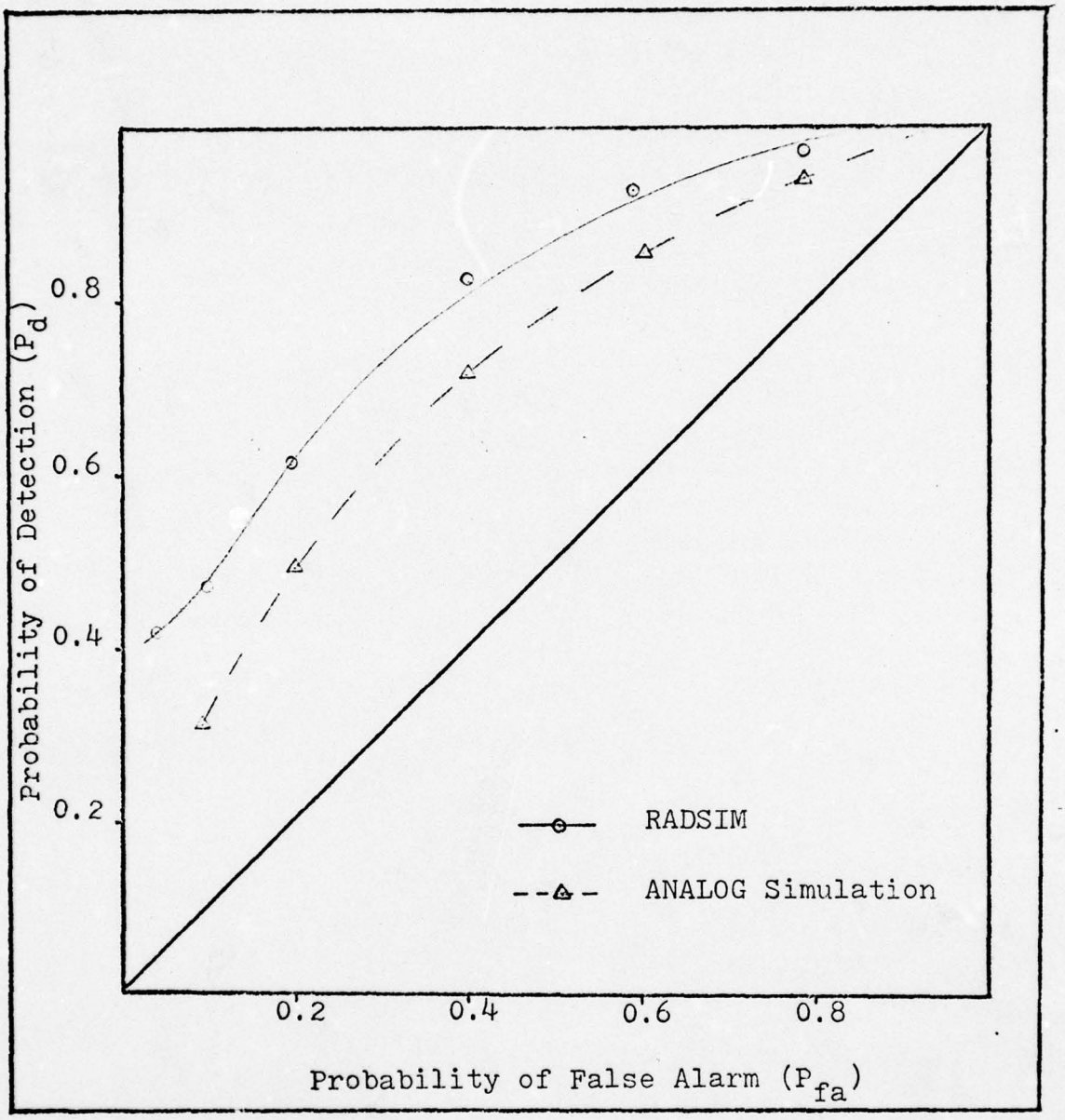

Figure 34. Comparison of Average Post-Integration Performance in SPRN. RADSIM vs. ANALOG Simulation

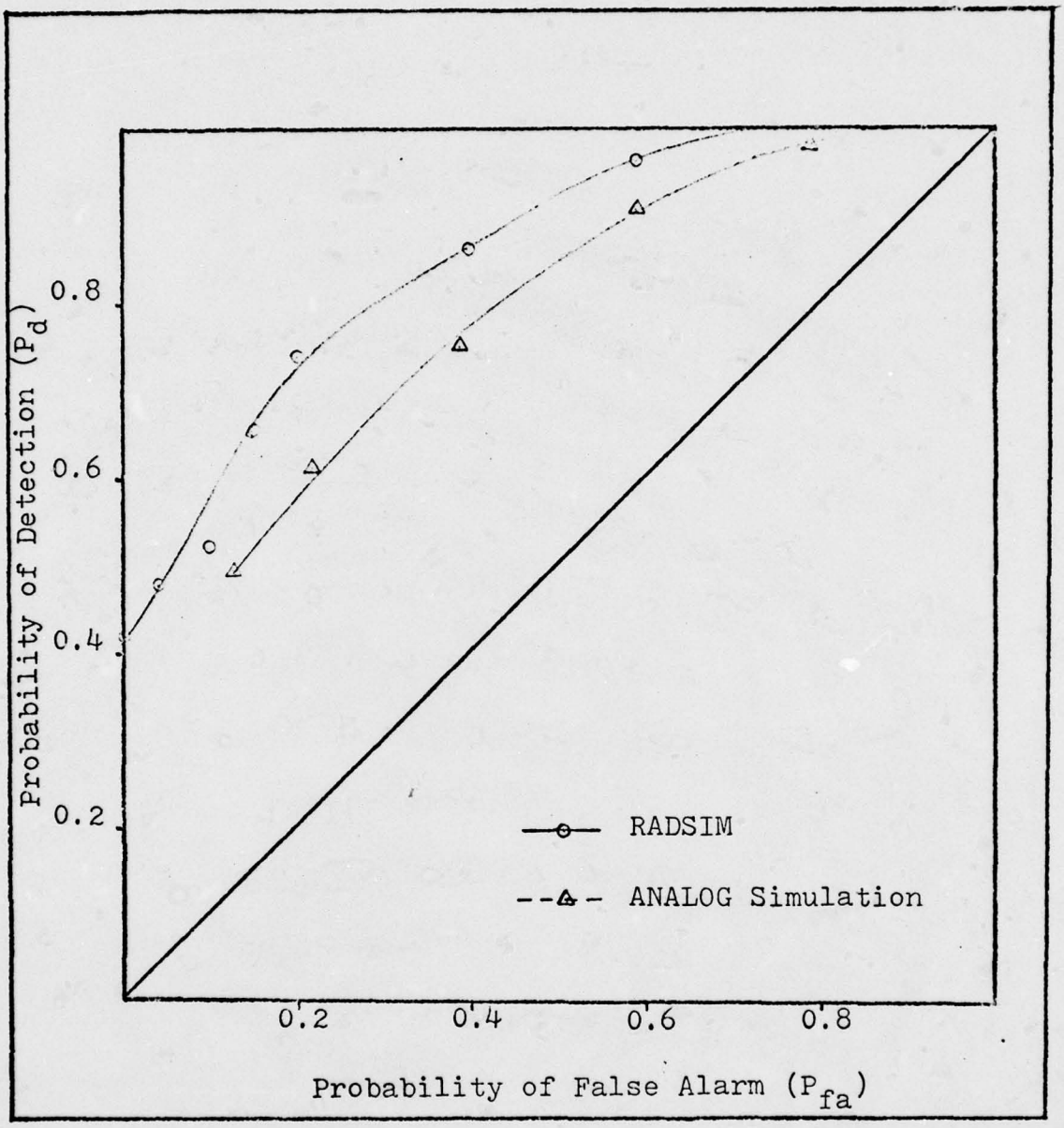

Figure 35. Comparison of the Average Pre-Integration Performance in SPRN. RADSIM vs. ANALOG Simulation

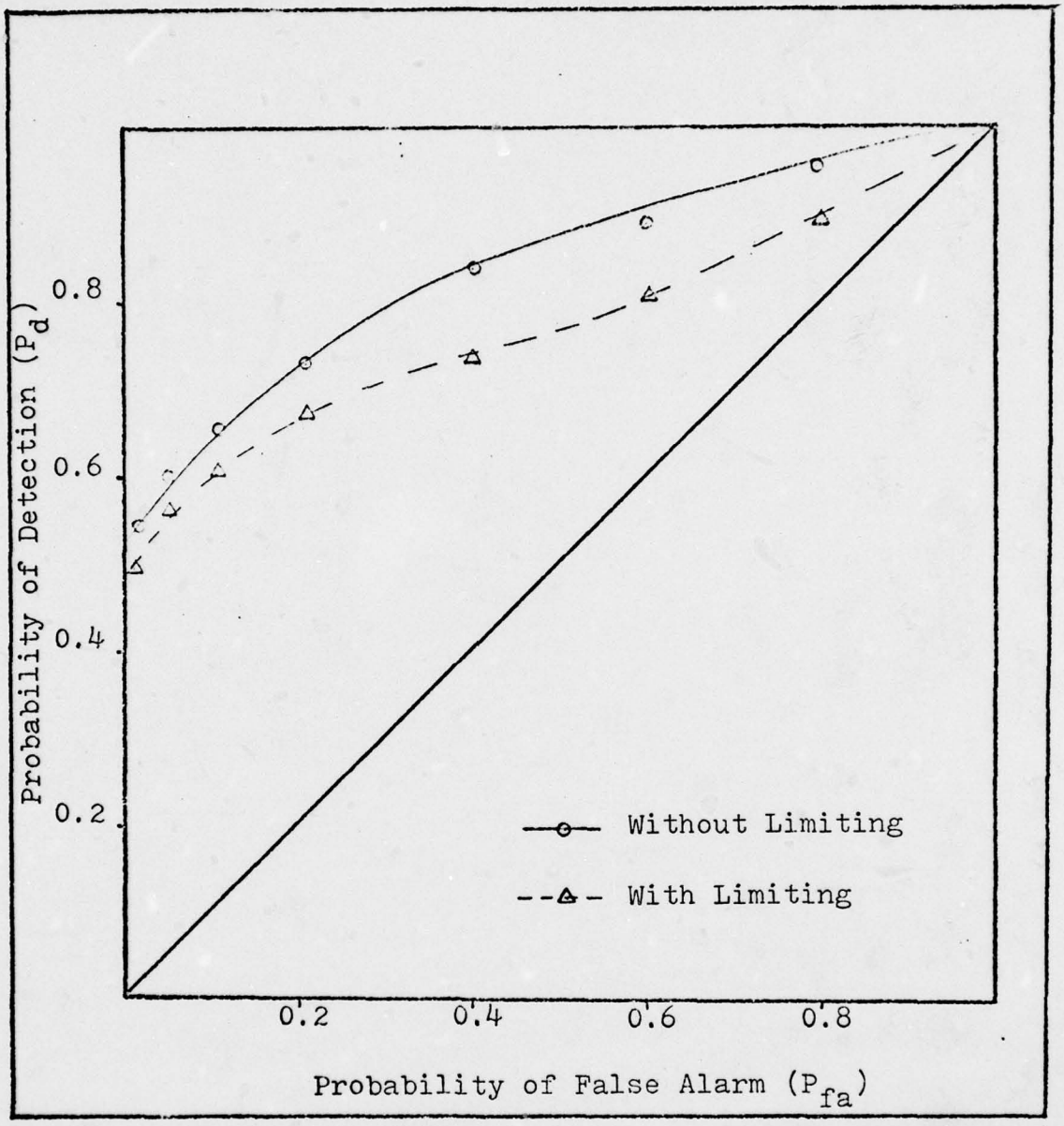

Figure 36. Comparison of Average Post-Integration Performance in WGN With and Without Limiting. SNR = 2

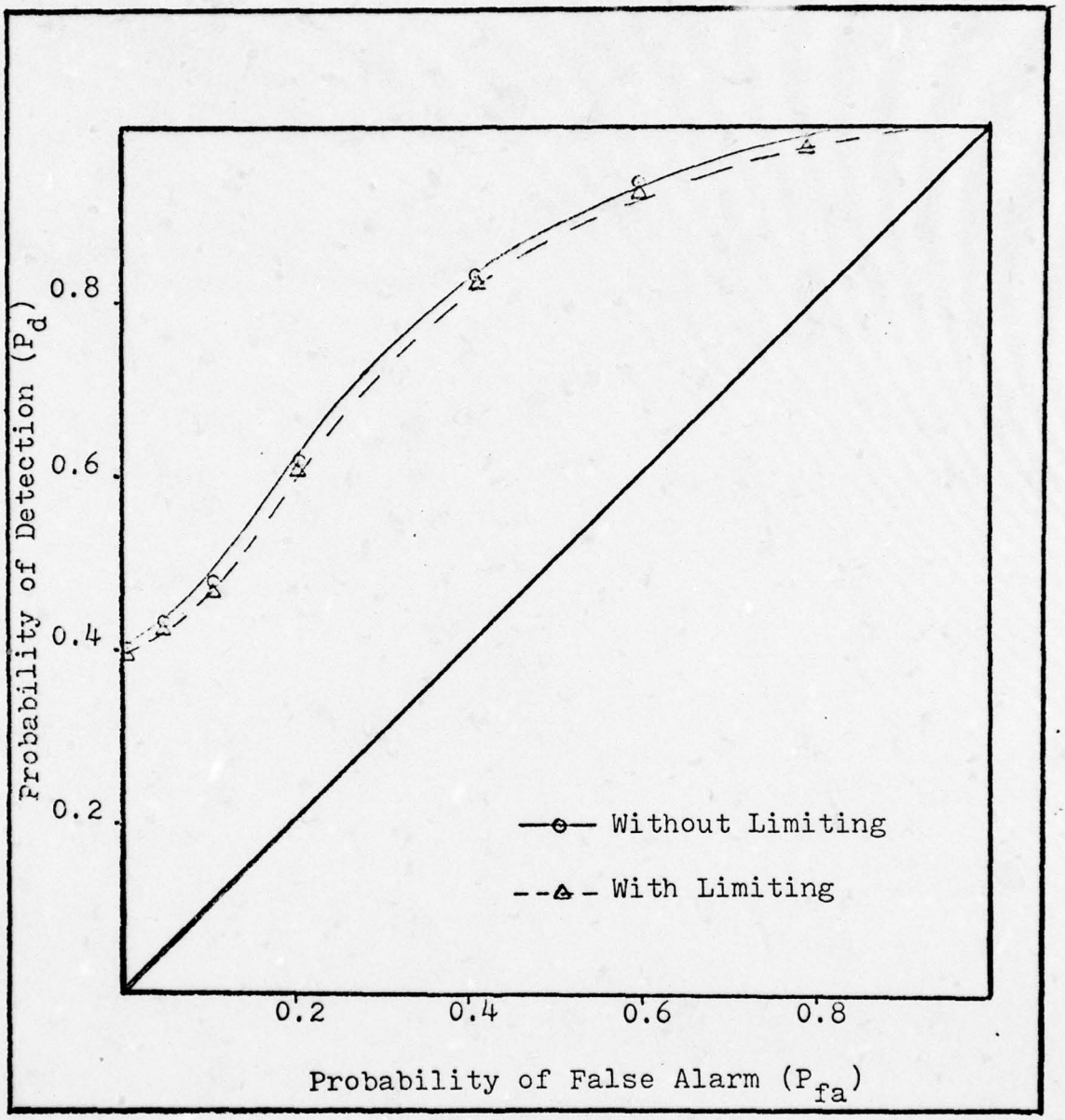

Figure 37. Comparison of Post-Integration Performance, With and Without Limiting, in Synchronized Pseudo-Random Noise.

were generally compatible with the theoretical development of Section II. An improvement in performance is evident when the receiver is operating in WGN, but performance degrades significantly in SPRN for approximately the same SNR.

The comparisons of performance between RADSIM results and the theoretical data developed by Berrie show a good correspondence for WGN and the same tendencies as Berrie for SPRN. The actual numerical differences are probably the result of differences in the actual signal to noise ratios used.

The use of a limiter did not demonstrate any performance improvement over the non limiting receiver. In the WGN cases a moderate performance degradation occurred as implied by Nathanson (Ref 7:122). In the SPRN case a very slight degradation was noted.

VI. Conclusions and Recommendations

The results described in Section V show that the original objectives of this thesis have been met. The RADSIM program has been successfully adapted to the ASD CDC 6600 computer system and shown to be a useful tool for the analysis of a search radar receiver. The results of Doctor Berrie's investigations of the effect of Pseudo-Random Noise on radar performance have been approximately duplicated, although an exact numerical correspondence was neither expected nor achieved. The use of a DICKE-FIX ECCM device has been shown to be ineffective against synchronized Pseudo-Random Noise Jamming of the form employed in this experiment.

Further studies are required to demonstrate the capabilities of SPRN jamming against other ECCM devices. Also, the spectral characteristics of subsequences of maximal length sequences should be investigated. The amount of energy in the bandwidth of the IF filter fluctuated greatly. In a range-gated radar receiver the target would appear in some range bins and be masked in others. Criteria should be developed for providing the masking in the range bins containing the target.

Bibliography

1. The University of Michigan. Electronic Countermeasures Institute of Science and Technology of the University of Michigan, 1961.

2. Berrie, David W. The Effects of Pseudo-Random Noise on Radar System Performance. ASD TR-74-23. Wright-Patterson Air Force Base, Ohio: Aeronautical Systems Division, 1974.

3. Hancock, Robert J. and F. H. Cleveland. Endo Atmospheric-Exo Atmospheric Radar Modelling. RADC TR-76-186, Volume I, Part 1. Griffiss Air Force Base, New York: Rome Air Development Center, 1976.

4. Berkowitz, Raymond S. Modern Radar. New York: John Wiley and Sons, Inc., 1965.

5. Berrie, David W. Table of Primitive Irreducible Modulus-Two Polynomials. ASD/ENAD TM-74-01. Wright-Patterson Air Force Base, Ohio: Aeronautical Systems Division, 1974.

6. Papoulis, Athanasios. Probability, Random Variables, and Stochastic Processes. New York: McGraw-Hill Book Co., 1965.

7. Nathanson, Fred E. Radar Design Principles. New York: McGraw-Hill Book Co., 1969.

8. Van Trees, Harry L. Detection, Estimation, and Modulation Theory. New York: John Wiley and Sons, Inc., 1968.

9. Control Data Corporation. FORTRAN Extended Version and Reference Manual. Publication No. 60305600, Revision G, Sunnyvale, California: Control Data Corporation, Publications and Graphics Division, 1975.

10. Aeronautical Systems Division. Subprogram Library Guide. Revision B. Wright-Patterson Air Force Base, Ohio: ASD Computer Center, 1976.

11. Johnson, David E. Introduction to Filter Theory. Englewood Cliffs, New Jersey: Prentice Hall, Inc., 1976.

12. Hancock, Robert J., and F. H. Cleveland. Endo-Atmospheric-Exo-Atmospheric Radar Modelling, Sample Problems. RADC TR-76-186, Volume I, Part 2. Griffiss Air Force Base, New York: Rome Air Development Center, 1976.

13. Hewlett Packard Incorporated. HP 3722A Operating and Service Manual. South Queensferry, West Lothian Scotland: Hewlett Packard Ltd., 1971.

14. Ziemer, R. E., and W. H. Tranter. Systems, Modulation, and Noise. Boston: Houghton Mifflin Company, 1976.

Appendix A

This appendix describes the program SPRNGEN used to provide samples of pseudo-random noise jamming for use in the RADSIM program.

Program Structure

SPRNGEN consists of a main program coded in FORTRAN, and an assembly language subroutine. The main program shown in Figure 38, reads the data which provides the parameters for the generator, sets up the required constants and calls the assembly language subroutine whenever a register shift is required. The assembly language subroutine, shown in Figure 39 shifts the register one bit and returns with the register sum (NCNT) and a bit of the pseudo-random code (NBIT). This sum is used to provide DSB modulation to a sampled carrier signal. Samples are written to TAPE3, and a count of the sums of the register states maintained.

Input Data

Data is read by a single list directed READ statement. Table IX lists the input data variables and their functions and restrictions, if any.

AD-A055 225 AIR FORCE INST OF TECH WRIGHT-PATTERSON AFB OHIO SCH--ETC F/G 17/4
AN APPLICATION OF SYNCHRONIZED PSEUDO-RANDOM NOISE TO RADAR JAM--ETC(U)
JAN 78 F E MOLINET

UNCLASSIFIED AFIT/GE/EE/78-12 NL

2 OF 2
AD
A055225

END
DATE
FILMED
7-78
DDC

Table IX
SPRNGEN Input Variables

CLKRT - The clock rate of the shift register.

SAMFRQ - The sampling frequency of the output signal. It must be equal to the simulation sample frequency FS.

CARFRQ - The carrier frequency of the jamming signal.

NSAMP - The number of samples desired. It must equal 2^{N2} where N2 is the same as the simulation variable.

N - The number of stages in the shift register.

MASK - The Feedback Mask of the shift register. It should be the decimal equivalent of a binary one in the position of each feedback tap.

NSEQ - The initial shift register state as a decimal number. It may not be zero.

TORIG - Not used.

```
      PROGRAM SPRNGEN(INPUT,OUTPUT,TAPE3)
      COMMON/IT1/IT,TORIG,DELT,TDUM,XT(8192)
      DIMENSION ISUM(60),JSUM(60),XTT(516)
      EQUIVALENCE (XTT(1),IT),(IT,NSAMP),(DELT,DELTIM)
      READ*,CLKRT,SAMFRQ,CARFRQ,NSAMP,N,MASK,NSEQ,TORIG
      NTTL=(2**N)-1
      DELTIM=1/SAMFRQ
      DELSHFT=1/CLKRT
      PI2=6.283185308
      TIME=0.0
      SHIFT=0.0
      DO 100 I=1,NSAMP
      IF(TIME.GE.SHIFT)GO TO 101
      GO TO 102
  101 CALL PN(N,MASK,NSEQ,NBIT,NCNT)
      ISUM(NCNT)=ISUM(NCNT)+1
      SHIFT=SHIFT+DELSHFT
  102 XT(I)=((NCNT-(N/2))*(COS(PI2*CARFRQ*TIME)))/(N/2)
  100 TIME=TIME+DELTIM
      NN=NSAMP+1
      WRITE(3) XTT
      IF(IT.GT.512)WRITE(3)(XT(J),J=513,IT)
      WRITE 1,IT
      WRITE 2
      WRITE 3,(I,ISUM(I),I=1,N)
      WRITE 4
      STOP
    1 FORMAT(* DATA STORED ON DATA SET 3  NPTS=*,I5)
    2 FORMAT(* STATISTICS OF DATA*,/,* NCNT*)
    3 FORMAT(60(1X,I2,3X,I5,/))
    4 FORMAT(* STATISTICS OF PRN*,/,* NCNT*)
    5 FORMAT(60(1H ,I2,3X,I8,/))
      END
```

Figure 38. SPRNGEN Main Program

```
          IDENT  PN
*
*         SUBROUTINE TO GENERATE A PSEUDO NOISE (PN) SEQUENCE.
*
*         CALL PN(N,MASK,NSEQ,NBIT,NCNT)
*
*         N      LENGTH OF THE SEQUENCE IN BITS.
*         MASK   FEEDBACK MASK.
*         NSEQ   PN SEQUENCE, MUST BE INITIALIZED NON ZERO.
*         NBIT   RIGHTMOST BIT OF NSEQ.
*         NCNT   NUMBER OF ONES IN NSEQ.
*
          ENTRY  PN
          BASE   0
          USE    CODE
*         A1     CONTAINS ADDRESS OF ARGUMENT LIST.
PN        BSS    1
          SA2    A1+1          GET MASK IN X2.
          SA2    X2
          SA3    A1+2          GET NSEQ IN X3.
          SA3    X3
          BX2    X2*X3         LOGICAL AND.
          CX2    X2            COUNT ONES IN X2.
          MX5    -1            GENERATE A ONE IN X5.
          BX5    -X5
          BX2    X2*X5         EVEN OR ODD NUMBER OF ONES.
          SA4    X1            GET N IN X4.
          SB4    X4
          LX2    B4            SHIFT LEFT N BITS.
          BX7    X3+X2         INCLUSIVE OR.
          AX7    1             SHIFT RIGHT ONE BIT.
          SA7    A3            RETURN NEW NSEQ.
          BX6    X5*X7         LOGICAL AND.
          SA2    A1+3          RETURN NEW NBIT.
          SA6    X2
          CX7    X7            NUMBER OF ONEW IN NSEQ.
          SA2    A1+4          RETURN NEW NCNT.
          SA7    X2
          JP     PN            RETURN.
          END
```

Figure 39. Assembly Language Subroutine

Vita

Fausto Edward Molinet, Jr., was born on 23 November 1940 in Richmond, Virginia. He graduated from High School in Cheyenne, Wyoming in 1959 and attended Virginia Military Institute and the University of Wyoming. He received the degree of Bachelor of Science in Electrical Engineering from the latter in May 1964, and received a commission in the USAF through the ROTC program. He then served as an Electronics Engineer and Staff Developmental Engineer in the Strategic Air Command and Air Force Systems Command until entering the School of Engineering, Air Force Institute of Technology in June 1975.

Permanent Address: 4014 Dunston Avenue
Richmond, Virginia 23225

This thesis was typed by Mrs. Sharon Maruna.

UNCLASSIFIED

SECURITY CLASSIFICATION OF THIS PAGE (When Data Entered)

REPORT DOCUMENTATION PAGE		READ INSTRUCTIONS BEFORE COMPLETING FORM
1. REPORT NUMBER AFIT/GE/EE/78-12	2. GOVT ACCESSION NO.	3. RECIPIENT'S CATALOG NUMBER
4. TITLE (and Subtitle) AN APPLICATION OF SYNCHRONIZED PSEUDO-RANDOM NOISE TO RADAR JAMMING		5. TYPE OF REPORT & PERIOD COVERED MS Thesis 6. PERFORMING ORG. REPORT NUMBER
7. AUTHOR(s) Fausto E. Molinet, Jr. Major USAF		8. CONTRACT OR GRANT NUMBER(s)
9. PERFORMING ORGANIZATION NAME AND ADDRESS Air Force Institute of Technology (AFIT-EN) Wright-Patterson AFB, Ohio 45433		10. PROGRAM ELEMENT, PROJECT, TASK AREA & WORK UNIT NUMBERS
11. CONTROLLING OFFICE NAME AND ADDRESS Test and Simulation Branch (ENADD) Defensive Avionics Division Aeronautical Systems Division Wright-Patterson AFB, Ohio 45433		12. REPORT DATE January 1978 13. NUMBER OF PAGES 100
14. MONITORING AGENCY NAME & ADDRESS (if different from Controlling Office)		15. SECURITY CLASS. (of this report) UNCLASSIFIED 15a. DECLASSIFICATION/DOWNGRADING SCHEDULE

16. DISTRIBUTION STATEMENT (of this Report)

Approved for public release; distribution unlimited

17. DISTRIBUTION STATEMENT (of the abstract entered in Block 20, if different from Report)

18. SUPPLEMENTARY NOTES Approved for public release; IAW AFR 190-17

JERRAL F. GUESS, Captain, USAF
Director of Information

19. KEY WORDS (Continue on reverse side if necessary and identify by block number)

Pseudo-Random Noise
Radar Simulation
ECCM/ECM
Radar Jamming

20. ABSTRACT (Continue on reverse side if necessary and identify by block number)

In 1974 Doctor David W. Berrie of Aeronautical Systems Division, proposed a radar jamming waveform derived from filtered pseudo-random binary sequences. The running time of the sequence is synchronized to the pulse repitition rate of the victim radar and defeats the post detection pulse integrator. Berrie's results were derived from theory and analog computer simulation. This study applies that waveform to a radar receiver model incorporating a DICKE-FIX (wide-band limiter) ECCM device and

DD FORM 1 JAN 73 1473 EDITION OF 1 NOV 65 IS OBSOLETE UNCLASSIFIED

SECURITY CLASSIFICATION OF THIS PAGE (When Data Entered)

uses a digital computer simulation (RADSIM) to determine radar performance. Berrie's results were essentially confirmed, and the DICKE-FIX device was found to be ineffective against this form of jamming.